



ALMA MATER STUDIORUM  
UNIVERSITÀ DI BOLOGNA

## ARCHIVIO ISTITUZIONALE DELLA RICERCA

### Alma Mater Studiorum Università di Bologna Archivio istituzionale della ricerca

Debris flows rainfall thresholds in the Apennines of Emilia-Romagna (Italy) derived by the analysis of recent severe rainstorms events and regional meteorological data

This is the final peer-reviewed author's accepted manuscript (postprint) of the following publication:

*Published Version:*

Ciccarese, G., Mulas, M., Alberoni, P.P., Truffelli, G., Corsini, A. (2020). Debris flows rainfall thresholds in the Apennines of Emilia-Romagna (Italy) derived by the analysis of recent severe rainstorms events and regional meteorological data. *GEOMORPHOLOGY*, 358, 1-21 [10.1016/j.geomorph.2020.107097].

*Availability:*

This version is available at: <https://hdl.handle.net/11585/960285> since: 2024-02-22

*Published:*

DOI: <http://doi.org/10.1016/j.geomorph.2020.107097>

*Terms of use:*

Some rights reserved. The terms and conditions for the reuse of this version of the manuscript are specified in the publishing policy. For all terms of use and more information see the publisher's website.

This item was downloaded from IRIS Università di Bologna (<https://cris.unibo.it/>).  
When citing, please refer to the published version.

(Article begins on next page)

# Debris flows rainfall thresholds in the Apennines of Emilia-Romagna (Italy) derived by the analysis of recent severe rainstorms events and regional meteorological data

Giuseppe Ciccacese <sup>a,\*</sup>, Marco Mulas <sup>a</sup>, Pier Paolo Alberoni <sup>b</sup>, Giovanni Truffelli <sup>c</sup>, Alessandro Corsini <sup>a</sup>

<sup>a</sup> University of Modena and Reggio Emilia, Department of Chemical and Geological Sciences, Via Giuseppe Campi 103, 41125 Modena, Italy

<sup>b</sup> Emilia-Romagna Region – ARPAE-SIM Regional Agency for Prevention, Environment and Energy, Viale Antonio Silvani 6, 40122 Bologna, Italy

<sup>c</sup> Emilia-Romagna Region – Regional Agency for Civil Protection and Territorial Security, Strada Giuseppe Garibaldi 75, 43121 Parma, Italy

## A B S T R A C T

Recent severe rainstorms events in October 2014 and September 2015 triggered more than a hundred debris flows in the western part of the Apennines of Emilia Romagna (Italy). In this work, we tested a novel method to define debris flows rainfall thresholds for the 2014 and 2015 rainstorms (which have been used as reference events) and to extend these results across the Apennines of Emilia Romagna, making use of long term rainfall data of the regional raingauges network. Results are compared, for validation, to rainfall rates recorded during other past rainstorm debris flows events (which have been used as validation events). At first, the method involves a spatial discriminant analysis between the spatial distribution of debris flows and the high frequency weather radar rainfall data for the 2014 and 2015 reference events. The analysis defines rainfall cutoff values over rainfall durations from 30' to 6 h, related to verification indices in the ROC curves, which are used as debris flows rainfall thresholds. Exceedance ratios are calculated between the computed rainfall thresholds and the rainfall rates at 10 years return periods at corresponding rainfall durations computed for raingauges located in the areas affected by the 2014 and 2015 events. The ratios are then used as multipliers of the rainfall rates at 10 years return periods over rainfall durations from 30' to 6 h calculated for all other raingauges in the regional study area. To spatialize thresholds calculation to the regional scale, the computed thresholds are interpolated across the Apennines of Emilia Romagna. The research resulted in the assessment of two levels debris flows rainfall thresholds curves which seem to be adequate to discriminate rainfall rates recorded during past debris flows events used for validation. Discussion evidences advantages and limits of our approach, compares results to existing debris flows thresholds and highlights their possible use in a multi stage warning procedure at regional scale.

**Keywords:**  
Debris flows  
Rainfall thresholds  
Weather Radar  
Raingauges

## 1. Introduction

Debris flows are potentially destructive landslide phenomena affecting many mountain areas of the world (Takahashi, 1991; Hung et al., 2001). In Italy, they are common in the Alps (Crosta and Frattini, 2001; Marchi et al., 2002; Floris et al., 2004; Marchi and D'Agostino, 2004; Berti and Simoni, 2007; Underwood et al., 2016) as well as in part of the central and southern Apennines (Fiorillo and Wilson, 2004; Giannecchini, 2005; Brunetti et al., 2010). In the Apennines of Emilia Romagna (i.e. the portion of the northern Apennines inside the administrative boundaries of Emilia Romagna Region), debris flows are much less frequent, both spatially and temporally, than other type of

landslides, such as earth slides and earth flows. Yet, a number of authors have reported their occurrence in the past (Moratti and Pellegrini, 1977; Papani and Sgavetti, 1977; Rossetti and Tagliavini, 1977). Also, recently, two Mesoscale Convective Systems causing rainstorms clusters in Parma province (October 2014) and in Piacenza province (September 2015) triggered more than a hundred debris flows (Corsini et al., 2017; Ciccacese et al., 2016; Ciccacese et al., 2017) and flash floods with large solid transport on the main watercourses (Scorpio et al., 2018). Both type of phenomena caused severe damages to infrastructures and a few casualties. The 2014 and 2015 events raised the interest of local public institutions for the assessment of debris flows warning thresholds in the Apennines of Emilia Romagna, since rainfall warning thresholds have so far been established only for slow to moderate velocity landslides by considering rainfall over time spans of days to weeks (Pignone et al., 2005; Pizzuolo et al., 2008; Martelloni et al., 2012; Berti et al., 2012; Segoni et al., 2015).

\* Corresponding author.

E-mail address: giuseppe.ciccacese@unimore.it (G. Ciccacese).

Debris flows thresholds are generally derived in intensity duration (I D) plots considering triggering rainfall over rainfall durations from few minutes to few hours (Guzzetti et al., 2008). This implies knowing the time of occurrence of the debris flows used in the analysis. In literature, a large number of authors have used I D plots for defining debris flows thresholds (Caine, 1980; Innes, 1983; Wieczorek, 1987; Jibson, 1989; Ceriani et al., 1994; Crosta and Frattini, 2001; Cannon and Gartner, 2005; Guzzetti et al., 2008). Some have also considered the influence of antecedent rainfall on the onset of debris flows (Govi et al., 1985; Corominas and Moya, 1996, 1999; Aleotti, 2004; Zêzere et al., 2005; Cardinali et al., 2006), while others have highlighted the importance of the representativeness of raingauge data on the identification of rainfall thresholds for debris flows with an I D approach (Nikolopoulos et al., 2014). Some authors have also highlighted the advantages of using weather radar data, which provide spatially continuous maps of rainfall intensity at high frequency, for the identification of debris flows thresholds (Nikolopoulos et al., 2015; Marra et al., 2014, 2017; Destro et al., 2017; Underwood et al., 2016). With reference to Italy, debris flows thresholds in I D plots have been proposed for some specific areas in the Alps (Paronuzzi et al., 1998; Deganutti et al., 2000; Genevois et al., 2000; Marchi et al., 2002; Bacchini and Zannoni, 2003; Aleotti, 2004; Floris et al., 2004; Gregoretto and Dalla Fontana, 2007) and in the central and southern Apennines (Guadagno, 1991; Calcaterra et al., 2000; Fiorillo and Wilson, 2004; Giannecchini, 2005). Recently, Peruccacci et al. (2017), by reviewing landslides thresholds over Italy, have also evidenced that in general, for many types of landslides, areas characterized by higher mean annual precipitations seem to be characterized by higher rainfall triggering thresholds. Actually, a number of authors have defined landslides thresholds by considering the deviations of triggering rainfalls from the ordinary precipitation regime of the analysed areas (Cannon, 1988; Crosta, 1998; Aleotti, 2004; Giannecchini, 2006; Giannecchini et al., 2012; Guzzetti et al., 2007; Bel et al., 2017).

In this work, we tested a novel method to define debris flows rainfall thresholds for the 2014 and 2015 rainstorm debris flows events (which have been used as reference events) and to extend these results across the Apennines of Emilia Romagna, making use of long term rainfall data of the regional raingauges network. Results are compared, for validation, to rainfall rates recorded during other past rainstorm debris flows events (which have been used as validation events). The motivation for not applying a conventional I D approach, is that the exact time of occurrence of the more than hundreds of debris flows occurred during the 2014 and 2015 MCS rainstorms is unknown, since debris flows took place in unmonitored basins. One of the specificities of the results, is that calculated debris flows thresholds have a geographical/climatic variability inside the regional study area, which is actually meant to take into consideration the dynamic geomorphic equilibrium of the debris condition in the river catchments to the precipitation and runoff climatology. The calculated thresholds have been compared to rainfall rates recorded during other debris flows events occurred in the past (in other areas of the region), and the validation results indicate that the computed spatially variable thresholds are substantially adequate to discriminate these past occurrences. Discussion evidences advantages and limits of our approach, compares results to existing debris flows thresholds and highlights their possible use in a multi stage warning procedure at regional scale.

## 2. Datasets

### 2.1. Debris flows occurrence

#### 2.1.1. Regional framework

The Apennines of Emilia Romagna extend for approximately 15.000 km<sup>2</sup>. The main reliefs are located along the SE NW watershed and reach a maximum elevation of 2165 m. Climate is generally "sub continental" and locally "cool temperate", according to the Köppen classification system. Annual rainfall varies from approximately

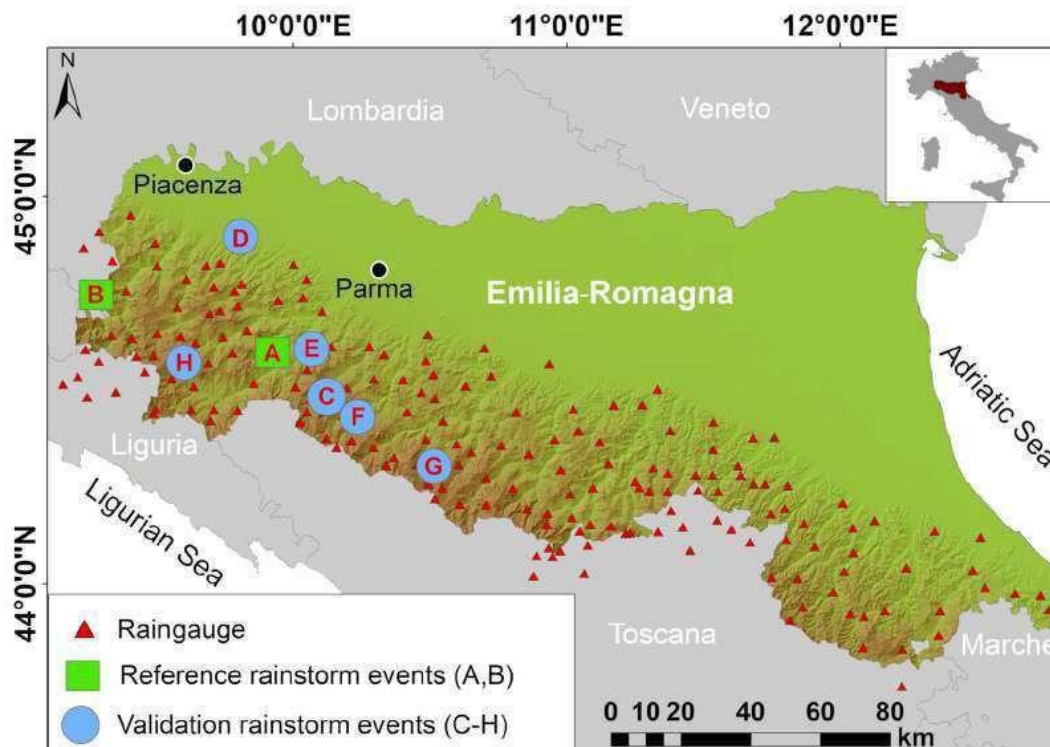


Fig. 1. Location of rainstorm events considered in this study which caused multiple debris flows in the period 1972 to 2016 (A, B: reference events; C–H: validation events) and position of 185 raingauges used in this study (located in the Apennines of Emilia-Romagna and nearby areas) (coordinates: WGS84–32N).

**Table 1**

List of rainstorm events considered in this study, which caused multiple debris flows in the period 1972 to 2016 (A, B: reference events; C–H: validation events).

Rainstorm event code	Date (dd/mm/yy)	Province (code)	Location	N° debris flows
A (reference)	13/10/2014	Parma (PR)	Parma and Baganza valleys	26
B (reference)	13–14/09/2015	Piacenza (PC)	Nure and Trebbia valleys	110
C (validation)	11/09/1972	Modena (MO) – Reggio Emilia (RE)	Secchia and Enza valleys	16
D (validation)	18/09/1973	Parma (PR)	Salsomaggiore Terme	1
E (validation)	16/10/1980	Parma (PR)	Corniglio	1
F (validation)	24–25/08/1987	Parma (PR) – Reggio Emilia (RE)	Ligonchio	1
G (validation)	25/10/2011	Modena (MO)	Tagliole in Pievepelago	1
H (validation)	05/11/2016	Parma (PR)	Case Mazzette in Albareto	2

1800 mm/year at the watershed to only 800 mm/year at the transition to the Po Plain, and it is mostly concentrated in autumn and spring. During winter a significant snow cover is deposited in the most elevated parts. Large convective rainstorms are generally occurring in late summer – early autumn. This part of the northern Apennines is characterized by the predominant presence of weak and highly fractured sedimentary rocks (Abbate et al., 1970; Bettelli and De Nardo, 2001) and by the presence of thousands of landslides, which are in most cases ascribable to slow moving complex earth slides and earth flows (APAT, 2007; Ronchetti et al., 2007; Trigila et al., 2015; Bertolini et al., 2017; Mulas et al., 2018; Piacentini et al., 2018).

Considering that in the Apennines of Emilia Romagna, every year, some tens of landslides are reported as being reactivated during the winter to spring period, debris flows have generally been considered less frequent, both spatially and temporally, than other type of landslides. Nevertheless, during 2014 in the province of Parma and 2015 in the province of Piacenza, two major rainstorms clusters caused by Mesoscale Convective Systems, triggered altogether as many as 136 debris flows (reference rainstorms events A and B in Fig. 1 and Table 1). On the other hand, altogether, the historic landslide database for Emilia Romagna (Piacentini et al., 2018) and other published documents (Moratti and Pellegrini, 1977; Papani and Sgavetti, 1977; Rossetti and Tagliavini, 1977; Tavaglini, 1989; Pasquali, 2003) and technical reports, include records of (only) 79 debris flows which have occurred in the past decades. Out of these, only 39 debris flows are referred to a specific day of occurrence and, out of these, only 22 debris flows (covering the period 1972 to 2016) can unequivocally be ascribed to rainstorms events which took place on the same day of occurrence (validation rain storms events C to H in Fig. 1 and Table 1).

### 2.1.2. Debris flows occurrence in the Parma 2014 and Piacenza 2015 events (reference events A and B)

The occurrence of debris flows in Parma province (October 13th 2014) and Piacenza province (September 13th to 14th 2015) was related to the development of large Mesoscale Convective Systems (MCS) causing thunderstorm clusters resulting in severe and persistent rainstorms. The MCS of October 13th 2014 in the upper valleys of Parma river and the Baganza torrent (reference event A) lasted for approximately 8 h (7:00–15:00, GMT + 1) (Cicarese et al., 2016; Corsini et al., 2017). The MCS of September 13th to 14th 2015 in the upper valleys of Nure, Trebbia and Aveto rivers (reference event B) lasted for approximately 6 h (22:00–04:00, GMT + 1) (Cicarese et al., 2017; Scorpio et al., 2018). Rainfall rates recorded during these events are presented in Section 2.2.

An inventory of a total of 136 debris flows was compiled soon after Event A (26 debris flows in 200 km<sup>2</sup>, Fig. 2a) and Event B (110 debris flows in 350 km<sup>2</sup>, Fig. 2b). In both cases, the most likely debris flows initiation points and the boundaries of the deposits were mapped in GIS. For reference event A, the inventory was based on field surveys carried out in the first weeks after the event and comparison to antecedent orthophotos of 2011. For reference event B, the inventory was based on field surveys as well as on the interpretation of post event

orthophotos acquired on 25th September 2015 (at 0.2 m resolution) and satellite images acquired from 18th to 21st September 2015 ([http://emergency.copernicus.eu/mapping/list\\_of\\_components/EMSR136](http://emergency.copernicus.eu/mapping/list_of_components/EMSR136)), and their comparison to antecedent pre event orthophotos of 2011. All of the inventoried debris flows showed deposits fresh enough and non vegetated as to be quite certainly ascribable to an occurrence during the periods of intense precipitations of the 2014 and 2015 MCS events. The assessment was also supported by the fact that the fresh features and deposits were not present in antecedent pre event orthophotos of 2011. On such basis, we know quite certainly that the mapped debris flows occurred during the period of the rain storm events A and B, but unfortunately, we do not have the specific information on the time of occurrence of each of the 136 debris flows, as they all took place in unmonitored basins located all over the affected valleys.

The inventory of 136 debris flows covers all the remote areas of the valleys and can be considered spatially rather complete. However, it is possible that some small undetected debris flows might be missing. The inventory includes both “mature debris flows” and “immature debris flows” (Takahashi, 1991), otherwise known as “debris flows” and “debris floods” (Hungr et al., 2001). The majority of the inventoried debris flows were channelized debris flows on slope incisions or creeks along quite densely vegetated slopes (Fig. 3). The initiation zones prevalently correspond to slope rotational failures or to points along the channels where deposits were remobilized. The involved material was mostly coarse granular debris and blocks of sandstones and limestones derived by the weathering of heterogeneous weak rocks such as Flysch (with high lithic/pelite ratio) in some cases alternated to block in matrix clayey shales (lithological classes Bl, Blp and APA in Figs. 1 and 2). Along the debris flow channels, evidences of streambed scouring, lateral erosion, erosion of materials previously trapped above check dams, and levees with inverse gradation were observable (Cicarese et al., 2016; Corsini et al., 2017). The accumulation zones, in most cases, were located at sudden slope profile changes or on small debris fans at the confluences of debris flows into the main streams or watercourses.

### 2.1.3. Debris flows occurrence in other past events (validation events C to H 1972 to 2016)

From the historic landslide database of Emilia Romagna, as well as from other documents and recent reports (Moratti and Pellegrini, 1977; Papani and Sgavetti, 1977; Rossetti and Tagliavini, 1977; Tavaglini, 1989; Piacentini et al., 2018), a database of 22 debris flows occurred during 6 specific severe rainstorms events in the period 1972 to 2016 (events C to H) has been used as validation dataset for the computed debris flows thresholds. Their location is reported in Fig. 1, while rainfall rates recorded these events are in Section 2.2.

The validation rainstorm event C (Modena and Reggio Emilia provinces, September 11th 1972) has been described by Moratti and Pellegrini (1977) and by Rossetti and Tagliavini (1977). The authors

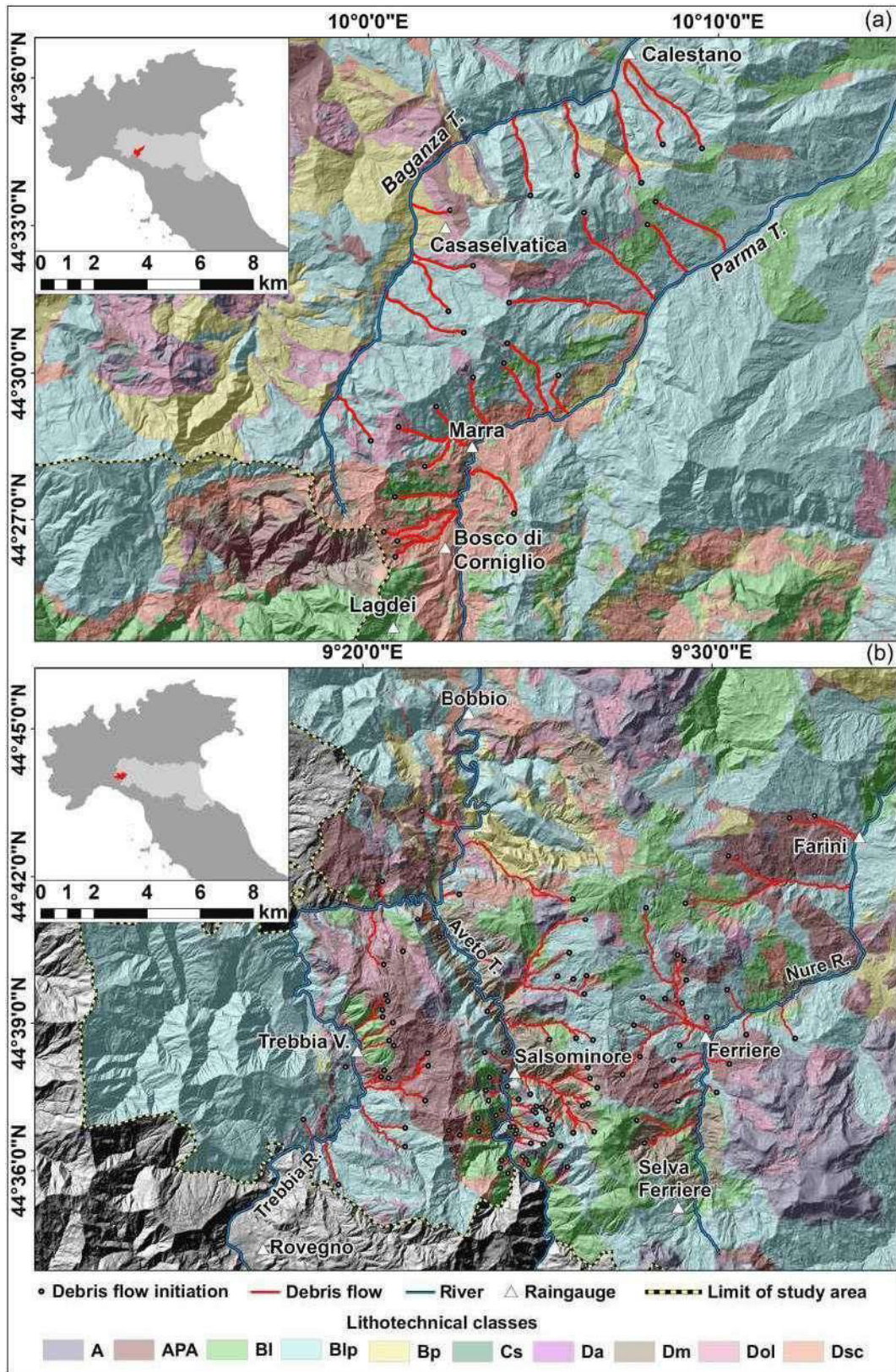


**Fig. 2.** Debris flows inventory compiled for: (a) Reference event A (Parma province, 13th October 2014). (b) Reference event B (Piacenza province, 13th–14th September 2015) (modified after: Ciccarese et al., 2016; Corsini et al., 2017). Keys to bedrock lithologies: A: Homogeneous hard rocks; BI: Heterogeneous weak rocks (Flysch, lithic/pelite ratio > 3); Blp: Heterogeneous weak rocks (Flysch, lithic/pelite ratio 0,3 ÷ 3); Bp: Heterogeneous weak rocks (Flysch, lithic/pelite ratio < 0,3); Cs: Weakly cemented Sandstones; Dm: Marls; Da: Clayey shales; Dol: Sedimentary block-in-matrix clayey shales; Dsc: Tectonic block-in-matrix clayey shales; APA: Heterogeneous weak rocks alternated to block-in-matrix clayey shales (coordinates: WGS84-32N).

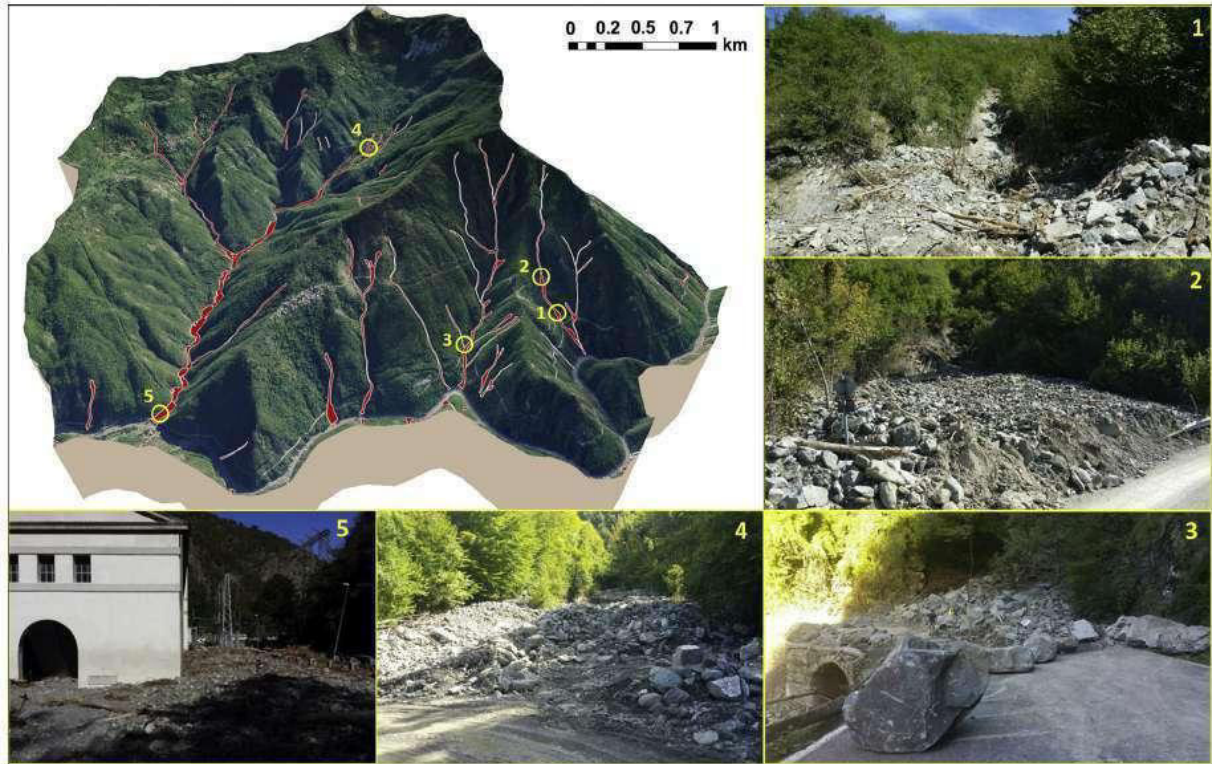


Fig. 3. Example of area affected by multiple debris flows during the 13th–14th September 2015 in Piacenza (reference event B), and pictures of debris flows phenomena a few days after the event. Note that the pictures have variable scales and are prospective: for reference, volume of larger pictured sandstones blocks is up to 1 m<sup>3</sup>.

describe the occurrence of a large MCS lasting several hours causing widespread debris flows and flash floods. They provide maps and pictures that have allowed us to locate 16 debris flows similar to these occurred during the reference events.

The validation rainstorm event D (Parma province, September 18th 1973) has been described by Papani and Sgavetti (1977). They refer to a major rainstorm in the morning and a second but less intense rainstorm in the afternoon. The event caused landslides, as well as flash floods on some torrents: in particular, the description provided for the flash flood along Rio Ghiare, indicates the occurrence of an immature debris flows along that torrent.

The validation rainstorm event E (Parma province, October 16th 1980) has been described by Tavaglini (1989). The author reports of diffuse damages due to mixed alluvial slope phenomena caused by a three days rainfall event peaked on October 16th. Considering the description provided by the authors, it is probable that several debris flows might have taken place during such event. Unfortunately, only one debris flow is pictured and expressly located along Rio d'Agna, which appears to have had characteristics similar to these occurred during reference events.

The validation rainstorm event F (Parma Reggio Emilia province, August 24th–25th 1987) has also been described by Tavaglini (1989). The author reports of persistent rainstorms during the night affecting large areas of the upper Apennines between the provinces of Parma and Reggio Emilia. The description is compatible with the actual occurrence of thunderstorms clusters during a MCS. They also report of several landslides and rockfalls affecting roads and threatening houses. However, out of their description, we have been able to locate only one debris flow near the village of Ligonchio.

The validation rainstorm event G (Modena province, October 25th 2011) is known on the basis of news from local newspapers and recent unpublished technical reports. It refers to a single specific debris flow occurred along a small creek in a steep wooden slope, which was triggered during persistent intense rainfalls related to thunderstorms clusters. The location and characteristics of the debris flows are known quite

precisely, since it affected a local road and it is clearly detectable on aerial photographs of November 2011.

The validation rainstorm event H (Parma province, November 5th 2016) is known on the basis of news from local newspapers and recent unpublished technical reports. It refers to a series of intense thunderstorms that triggered a debris flow that invaded and interrupted a local road. The debris flow has been mapped quite precisely in the field, and it is actually also visible on post-event Google Earth images.

## 2.2. Rainfall data

### 2.2.1. Raingauges data (maximum rainfall rates at various rainfall durations) during the Parma 2014 and Piacenza 2015 debris flows events (reference events A and B)

Rainfall Total (RT) at 30' frequency in the areas affected by Parma 2014 and Piacenza 2015 events (reference events A and B) have been collected from raingauges which are part of the ARPAE SIM network, which are made available for the period year 2000 to date in an open access portal (<https://simc.arpae.it/dext3r>, in Italian language only).

Representative histograms of rainfall during events A and B are presented in Fig. 4, while maximum cumulated rainfall (mm) at various rainfall durations (and the corresponding return periods) recorded by all of the raingauges in the areas affected by events A and B are presented in Table 2.

For instance, at the centre of the MCS area during reference event A, the rain gauge of Marra recorded 302.8 mm in 24 h, with max rainfall intensity between 7:00 and 15:00 of 13th October, with peaks of 31.2 mm/15' and 82 mm/1 h, a value with >200 years return period (Fig. 4a). Similar rates were recorded by other raingauges in the MCS area (Table 2). On the other hand, at the centre of the MCS area during reference event B, the rain gauge of Salsominore, recorded 328.4 mm in 24 h, with maximum intensity between 22:00 of 13th and 03:00 of 14th September, during which the 6 h precipitation reached 307.4 mm and

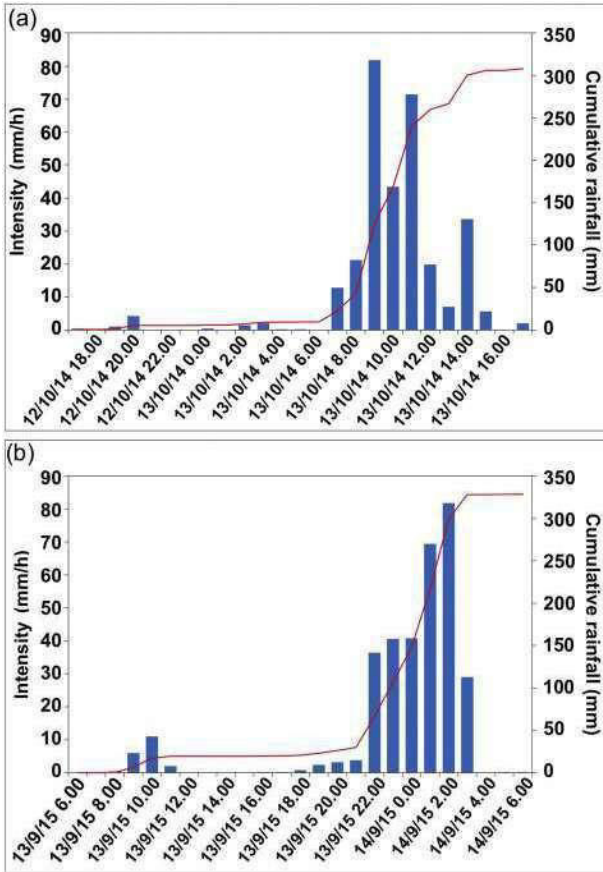


**Fig. 4.** Histogram of rainfall recorded by raingauges during: (a) Reference event A (Parma province, 13th October 2014: raingauge of Marra). (b) Reference event B (Piacenza province, 13th–14th September 2015: raingauge of Salsominore). (Modified after Ciccarese et al., 2016 and Corsini et al., 2017).

maximum reached 32,2 mm/15' and 107.6 mm/1 h (Fig. 4b). Even higher values, associated to return periods of >200 years, were recorded by other raingauges in the rainstorms area (Table 2).

### 2.2.2. Raingauges data (maximum rainfall rates at various rainfall durations) during other past debris flows events (validation events C to H 1972 to 2016)

For validation debris flows events occurred after year 2000 (i.e. validation events H and H), data regarding the maximum intensity of rainfall over different rainfall durations (Table 3) have been obtained by using Rainfall Total (RT) cumulated over 30' in raingauges which are part of the ARPAE SIM network. As mentioned for reference events A and B, RT data are available for the period year 2000 to date, by accessing an open access portal (<https://simc.arpae.it/dext3r>, in Italian language only).

For validation debris flows events occurred before year 2000 (i.e. validation events C to F, for which RT data are not available) data regarding the maximum intensity of rainfall over different rainfall durations (Table 3) have been obtained by the Hydrological Annals of raingauges in the ARPAE SIM network. The Hydrological Annals are available for years from 1930 to date, by accessing an open access portal ([https://www.arpae.it/sim/?idrologia/annali\\_idrologici](https://www.arpae.it/sim/?idrologia/annali_idrologici), in Italian language only). The Annals include records of the Yearly Rainfall Maxima (YRM) reached over rainfall durations of 1, 3, 6, 12, 24 h. Actually, in the years of occurrence of validation events C to F and in raingauges located in the areas affected by debris flows, the YRM at 1, 3, 6 h were reached on the same day of occurrence of debris flows, allowing us to determine the maximum rainfall rates associated to the validation events. As presented in the Methods section, the data collected in

Table 3 have been used to validate the results of the thresholds assessment procedure.

### 2.2.3. Weather radar data (spatially distributed ground rainfall rates at 30') during Parma 2014 and Piacenza 2015 debris flows events (reference events A and B)

Two datasets of gauge adjusted Surface Rainfall Total (SRT) cumulated at 30' intervals from the Italian weather radar network (Alberoni et al., 2002) have been collected for reference events A (Parma 2014) and B (Piacenza 2015). Datasets have been provided by the National Department of Civil Protection (NDCP) and derive from the integration of data from 6 weather radars, two of which located in Emilia Romagna (Fig. 5a). The estimates of rainfall at the ground in the SRT datasets at 30' have been adjusted by NDCP on the basis of data from the dense network of raingauges spread all over Italy, including these of the ARPAE SIM network presented in the previous paragraph. The adjustment procedure is based on a conditional merging procedure that makes use of an adjustment matrix containing a dynamic multiplier coefficient, which is calculated at specific time intervals (in this case 30') on the basis of the ratio between the cumulated rainfall recorded by the radars and the cumulated rainfall in raingauges, interpolated using the GRISO model (Pignone et al., 2010).

Like any radar rain gauge data merging method, this procedure might have resulted in rainfall estimates affected by some uncertainties (Ochoa Rodriguez et al., 2019). The SRT datasets for event A and B have been provided by the NDCP as a series of georeferenced raster maps at  $1 \times 1$  km spatial resolution representing the spatial distribution of 30' cumulated rainfall at the ground. The datasets cover the duration of the events A and B, so that cumulated rainfall in any time interval can be obtained by summing up data in individual STR 30' maps (see Fig. 5b, c). As it will be presented in the Methods section, this dataset has been used to derive asynchronous rainfall maxima maps at various rainfall durations.

### 2.2.4. Raingauges data (long term Yearly Rainfall Maxima) across the Apennines of Emilia Romagna

As mentioned in Section 2.2.2, the Yearly Rainfall Maxima (YRM) over rainfall durations of 1, 3, 6, 12, 24 h, are available from hydrological annals of raingauges in the ARPAE SIM network that cover the long term period from 1930 to date ([https://www.arpae.it/sim/?idrologia/annali\\_idrologici](https://www.arpae.it/sim/?idrologia/annali_idrologici)). We have collected YRM data for 185 raingauges (out of the 210 raingauges available in total), for which long term time series of YRM covered at least 13 years out of the last 20 years (so that YRM data are representative also of recent meteorological conditions). For individual raingauges, the length of collected time series of YRM range from 88 to 13 years. The YRM data referring to validation debris flows events occurred prior to year 2000 (see Section 2.2.2) are a subset of this dataset. As presented in the Methods section, the long term YRM data series have been used to assess rainfall rates for 10 years return period over rainfall durations from 30' to 6 h for each of the 185 raingauges selected.

## 3. Methods

### 3.1. Rationale

As mentioned in the introduction, a large number of authors have proposed debris flow thresholds at national to regional scale which are based on simple deterministic approaches that draw a lower envelope to triggering rainfalls in an Intensity Duration plot, once the exact time of occurrence of the debris flows is known so to associate to the debris flows the exact antecedent rainfall rates over different rainfall durations. The reason why we have decided not apply a similar deterministic I D approaches to define a specific lower envelope for debris flows triggering in the Apennines of Emilia Romagna, is that no data is available regarding the exact time of occurrence for the 136 debris flows mapped

**Table 2**

Maxima cumulated rainfalls at various rainfall durations and corresponding return periods recorded by raingauges during: (a) Reference event A (Parma province, 13th October 2014). (b) Reference event B (Piacenza province, 13th–14th September 2015). (Note: the length of the record used to calculate the return periods and the calculation method are reported in Section 2.2.3).

Reference Event A		Maximum cumulated rainfall (mm) from 17:00 of 12/10/2014 to 17:00 of 13/10/2014							
Raingauge	Elevation (m)	15'	30'	1 h	2 h	3 h	6 h	12 h	24 h
Bosco di Corniglio	908	30,2	52,8	72,6	115,2	160	213,6	253	261
Calestano	384	11,6	19,4	36,8	58	74	116,2	138,2	139,8
Casaselvatica	830	7	13,8	27	48,4	66,2	97,2	129	132,4
Lagdei	1247	29,8	51	69,4	106,6	144,4	196	229,6	237,8
Marra	626	31,2	58,2	82	132	196,6	257,8	298,8	302,8
Reference Event A		Return period of Maximum cumulated rainfall (years)							
Raingauge	Elevation (m)	15'	30'	1 h	2 h	3 h	6 h	12 h	24 h
Bosco di Corniglio	908	17	113	157	>200	>200	>200	103	23
Calestano	384	2	2	6	16	33	82	66	35
Casaselvatica	830	1	1	2	35	10	12	10	5
Lagdei	1247	5	13	19	16	18	12	7	3
Marra	626	14	>200	>200	>200	>200	>200	>200	>200
Reference Event B		Maximum cumulated rainfall (mm) from 06:00 of 13/09/2015 to 06:00 of 14/09/2015							
Raingauge	Elevation (m)	15'	30'	1 h	2 h	3 h	6 h	12 h	24 h
Bobbio	272	9,6	18,6	30,2	58,8	77,6	103,2	103,6	115
Farini	436	17,4	29,8	52,4	86,2	113,4	168,4	169,2	176,8
Ferriere	656	28,8	54,2	87,6	129,4	150	237,6	238	253,6
Rovegno	745	36,8	71,4	116	142	177,4	266	267	296,2
Salsominore	408	32,2	57,2	107,6	151,2	201,8	307,4	308,6	328,4
Selva Ferriere	1109	16,6	30,4	51,8	77	91,6	176,4	188,4	209,8
Trebbia Valsigara	462	28,2	48,6	89,6	139,8	176,6	238,6	239,2	255,4
Reference Event B		Return period of Maximum cumulated rainfall (years)							
Raingauge	Elevation (m)	15'	30'	1 h	2 h	3 h	6 h	12 h	24 h
Bobbio	272	1	2	4	44	133	>200	86	25
Farini	436	5	12	141	>200	>200	>200	>200	133
Ferriere	656	7	47	>200	>200	>200	>200	>200	>200
Rovegno	745	17	137	>200	>200	>200	>200	192	168
Salsominore	408	4	9	76	61	93	113	82	82
Selva Ferriere	1109	3	5	12	17	19	68	47	39
Trebbia Valsigara	462	6	8	66	75	58	56	42	37

after reference events A and B and, more so, for the other debris flows occurred during validation events C to H, because they took place in unmonitored basins.

At the same time, the adoption for the Apennines of Emilia Romagna of one of the already existing debris flows threshold curves proposed in literature, has to come to terms with the fact that proposed regional and local thresholds are significantly variable and that they do not take into consideration the meteorological characteristics of the various parts of this area that, somehow, might condition debris flows thresholds. In Fig. 6, for instance, regional and local debris flows thresholds included in the review paper of Guzzetti et al. (2007) are plotted against the maximum rainfall rates recorded during the A to H reference and validation rainstorms debris flows events occurred in the Apennines of Emilia Romagna from 1972 to 2016. The plot shows that the maximum rainfall rates recorded during the reference and validation rainstorms debris

flows events, tend to be much higher in locations (i.e. raingauges) characterized by higher values of rainfall rates for 10 years return period (represented with larger dots in Fig. 5). In other terms, the lower envelope of the maximum rainfalls reached during triggering events over the Apennines of Emilia Romagna would correspond to rainfall rates with return periods of <1 year in some parts of the region and to return periods of more than hundreds of years in others.

Consequently, the rationale of the discriminant analysis approach adopted in this research is founded on the assumption that a mid term dynamic geographic climatic equilibrium should exist between debris slope to stream bed states and the rainfall regime of the affected areas and that this, in turn, can be reflected on triggering rainfall thresholds. For instance, most of the debris flows during 2014 and 2015 reference events (as well as probably most of these reported during the validation events) were triggered by failure and mobilization of slope

**Table 3**

Maximum cumulated rainfall recorded over different rainfall durations by raingauges during validation events C to H.

Event	Date (dd/mm/yy)	Province (code)	Location	N° debris flows	Relevant raingauge	Max. rainfall (mm)				
						30'	1 h	2 h	3 h	6 h
C	11/09/1972	Modena (MO) – Reggio Emilia (RE)	Secchia and Enza valleys	13	Succiso	n.a.	97	n.a.	247	311
				1	Ospitaletto	n.a.	58	n.a.	111.6	147.2
				2	Lago Paduli	n.a.	102	n.a.	229.4	279
D	18/09/1973	Parma (PR)	Salsomaggiore Terme	1	Salsomaggiore	n.a.	71	n.a.	71	112
E	16/10/1980	Parma (PR)	Corniglio	1	Bosco di Corniglio	n.a.	50	n.a.	120	180
F	24–25/08/1987	Parma (PR) – Reggio Emilia (RE)	Ligonchio	1	Ligonchio	n.a.	98	n.a.	196	223
G	25/10/2011	Modena (MO)	Tagliole in Pievepelago	1	Pievepelago	17	29.4	53.8	71.6	119.2
H	05/11/2016	Parma (PR)	Case Mazzette in Albareto	2	Albareto	32.8	60.2	113	135.6	145.4

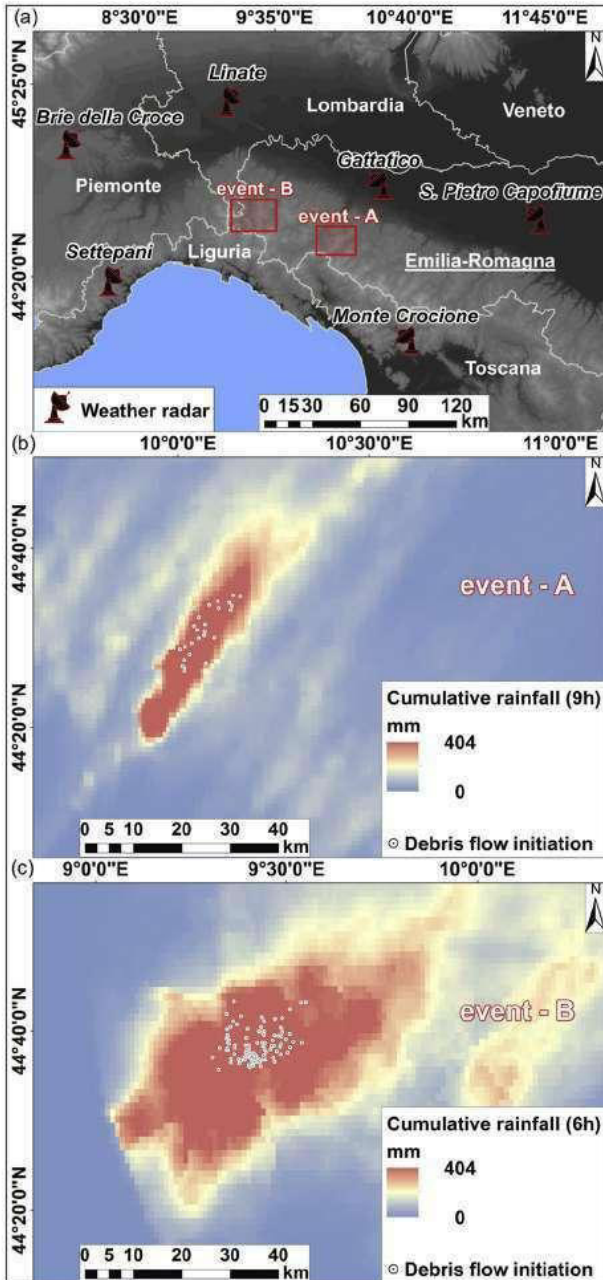


Fig. 5. (a) Distribution of weather radars used by the NDCP to estimate the rainfall during reference event A and reference event B; (b) Maps of cumulated rainfall from 07:00 to 16:00 of 13th October 2014 for reference event A; (c) Maps of cumulated rainfall from 22:00 of 13th and 04:00 of 14th September 2015 for reference event B (coordinates: WGS84-32N).

debris covers located close to, or along, creeks and impluvium areas. These deposits have a relatively little possibility to be mobilized under ordinary rainfall conditions (a situation which is indeed quite different from the channelized debris flows in the Dolomites which are constantly fed by rockfalls). Thus, debris failure and subsequent debris flows are most likely to occur as a consequence of “unusual” rainfall events, since “ordinary” rainfall events should have already mobilized the poorly stable debris in the past. On the other hand, the extent to which a given rainfall rate over a specific short rainfall duration can be considered “unusual”, is correlated to the rainfall rates that can be considered “ordinary”. It is expected that in areas of the Apennines of Emilia Romagna in which high rainfall rates at short rainfall durations are frequent (and consequently locally “ordinary”) debris flows triggering

thresholds should be higher than in areas with lower rates of frequent short duration. The potential limitations of this approach are commented in the Discussion section.

### 3.2. Operational procedures

#### 3.2.1. General framework

The main links between data sources and operational procedures are schematized in Fig. 7. The procedures start with a discriminant analysis between the spatial occurrence of debris flows and the spatial distribution of asynchronous rainfall maxima during the reference events A and B. The aim of discriminant analysis is to identify specific rainfall cutoff values (lower than the maximum reached) that, at different rainfall durations during events A and B, would have had higher capacity to discriminate the occurrence of DF (i.e. indirectly accounting for the most probable rainfall rate that did actually trigger them). Subsequently, to define a normalization metrics, the predictive cutoff values, at different rainfall durations, are ratioed to the corresponding rainfall rates for a given return period (using data from raingauges located inside the events A and B). The computed exceedance ratios are used to spatialize results, i.e. to compute threshold values for all hundreds of raingauges located in the region, by using the ratios as multiplier of the rainfall rates for a given return period on the rainfall durations considered. Results are finally spatialized by interpolation over the Apennines of Emilia Romagna, and are confronted with rainfall data from the past events C to H for validation.

#### 3.2.2. Debris Flows Initiation maps (DFI) (events A and B)

The information regarding the position of the initiation zones of debris flows during reference events A and B, has been used to derive two raster Debris Flows Initiation maps (DFI) at  $50 \times 50$  m resolution, in which a cell assumes value 1 if at least one debris flow triggering points falls into the raster cell (consequently one cell can include 1 or more initiation zones of debris flows).

#### 3.2.3. Asynchronous Rainfall Maxima maps at different rainfall durations (ARM<sub>j</sub>) (events A and B)

During reference event A and B, the maximum intensity of rainfall was reached asynchronously in different locations of the affected area. The SRT dataset at 30' frequency from the weather radar network was post processed in order to derive a series of Asynchronous Rainfall Maxima maps (ARM<sub>j</sub>) at different rainfall durations  $j$  (30', 1 h, 2 h, 3 h e 6 h), by using a 30' moving window over which the maxima of cumulated rainfall totals at various rainfall durations are extracted using GIS functionalities (Fig. 8).

#### 3.2.4. Discriminant ROC analysis and cutoff rainfall values of verification indices

The Receiver Operating Characteristic (ROC) is a broadly used method to assess the performance of discriminant forecast models (Swets, 1988). It has also been used in order to evaluate the performances of rainfall thresholds (Mathew et al., 2014; Gariano et al., 2015; Corsini and Mulas, 2016). We have applied this method to create ROC curves for reference events A and B, by performing a cell by cell comparison between DFI maps and ARPMs maps at  $j$ th rainfall durations 30', 1 h, 2 h, 3 h, 6 h. The contingency tables have been created by considering rainfall cutoff values at intervals of: 10 mm (for ARPMs at  $j = 30'$  and  $j = 1$  h); 20 mm (for ARPMs at  $j = 2$  h) and 30 mm (for ARPMs at  $j = 3$  h and  $j = 6$  h). Sensitivity analysis has shown that the influence on results of the intervals considered is actually quite limited (see Discussion section).

From each contingency table referring to a specific event (A or B) and to a given  $j$ th duration, a ROC curve has been calculated by

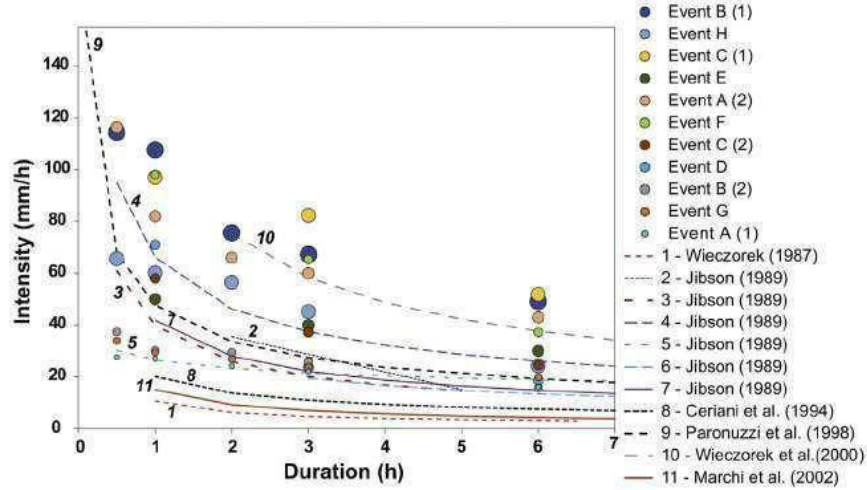


Fig. 6. Regional and local debris flows thresholds included in the review paper by Guzzetti et al. (2007), against the maxima rainfall rates during the A to H reference and validation rainstorms – debris flows events in the Apennines of Emilia-Romagna.

plotting the “TP rate” vs. the “FP rate” for each rainfall cutoff value.

$$\text{TP rate} = \text{TP}/(\text{TP} + \text{FN}); \text{FP rate} = \text{FP}/(\text{FP} + \text{TN}),$$

where TP (hits), FP (false alarm), FN (misses), TN (correct rejections).

The overall predictive capacity of the different  $j$ th rainfall durations has been assessed by calculating the area under the ROC curve (AUC). According to Swets (1988),  $\text{AUC} > 0.7$  indicates moderately accurate models while  $\text{AUC} > 0.9$  indicates highly accurate models.

Moreover, in each ROC curve, the discriminant performance of each cutoff rainfall value has been assessed by using verification indices. Among the many available in literature, we considered the “distance from top left corner” (DIS, ranging 0 to 1) and the “critical success index” (CSI, ranging 0 to 1, also known as “threat score”).

$$\text{DIS} = \sqrt{(1 - \text{TP rate})^2 + (\text{FP rate})^2}; \text{CSI} = \text{TP}/(\text{TP} + \text{FN} + \text{FP}).$$

An ideal predictor would have  $\text{DIS} = 0$  and  $\text{CSI} = 1$ .

The DIS has been selected since, when at its minima, it represents the indices that maximizes the ratio between TP\_rate and FP\_rate, i.e. that is capable of predicts the most hits (i.e. debris flows) with the minimum false alarms. The CSI, on the other hand, has been selected as it is not affected by the number of non event forecasts. By definition, the cutoff values in the ROC curve for the relative minimum DIS are bound to be lower than the cutoff values for the maximum CSI. The CSI is a biased score that dependent upon the frequency of the events. In our case, the consequence of having a limited number of positive events (i.e. pixels corresponding to debris flows) compared to the total of the pixels in the ARPMs maps, is that the computed values of CSI are always extremely low for all cutoff values. However, this is not a problem biasing our analysis, as the selection of rainfall cutoff values to be used as threshold has been based on the relative maximum CSI in each ROC curve.

For event A and B, from each ROC curve for rainfalls at  $j$ th rainfall durations (30', 1 h, 2 h, 3 h, 6 h), we have therefor retrieved the rainfall cutoff values for the minimum DIS ( $P_{\text{DIS-event-A}(j)}$ ;  $P_{\text{DIS-event-B}(j)}$ ) and the maximum CSI ( $P_{\text{CSI-event-A}(j)}$ ;  $P_{\text{CSI-event-B}(j)}$ ). Since, expectedly, the  $P_{\text{DIS}(j)}$  values are lower than the  $P_{\text{CSI}(j)}$  at any  $j$ th rainfall duration considered, rainfall cutoff values  $P_{\text{DIS}(j)}$  can be considered as lower rainfall thresholds for discriminating debris flows occurrences and the  $P_{\text{CSI}(j)}$  as higher rainfall thresholds for discriminating debris flows occurrences. It should also be mentioned that rainfall cutoff values for min. DIS and max CSI are always lower than maximum rainfall values represented in the ARPMs.

### 3.2.5. Computation of rainfalls rates for 10 years return periods in specific $j$ th rainfall durations

The rainfall rate at 10 years return period ( $P_{\text{RP10}(j)}$ ) for  $j$ th rainfall durations of 30', 1 h, 2 h, 3 h, 6 h, has been calculated for each of the 185  $i$ th raingauge of the ARPAE network distributed across the Apennines of Emilia Romagna by using time series of YRM and conventional methods for rainfall depth duration frequency (DDF) analysis (Chow et al., 1988). Time series of YRM ranged from 85 years to 13 years. All the time series had at least 13 years of data in the last 20 years. Relatively short time series are not optimal for calculation of  $P_{\text{RP10}(j)}$ . However, excluding raingauges with shorter time series would have reduced the spatial density of raingauges considered in the analysis. Moreover, the shorter YRM time series are referring to recently installed raingauges of the ARPAE SIM network which are used for thunderstorms warning, and also for this reason we decided to include them in the analysis. The method used to estimate  $P_{\text{RP10}(j)}$  by using rainfall depth duration frequency (DDF) analysis for each raingauge is substantially described in Di Baldassarre et al. (2006), and it is based on the Gumbel extreme value probability distribution type 1 (Gumbel, 1958). The Gumbel probability distribution parameters “ $\alpha$ ” and “ $u$ ” for rainfall durations of 1 h, 3 h, 6 h, 12 h, 24 h, have been determined for each raingauge by the method of moments, by relating them to the mean  $\mu(x)$  and standard deviation  $\sigma(x)$  of YRM time series with:

$$\alpha_i = 1.283 \times \sigma(x); u_i = \mu(x) - 0.450 \times \sigma(x).$$

On such basis, for each raingauge, it has been possible to assess, for any return period (RP), the rainfall quantile ( $x_t$ ) over the different rainfall durations (1 h, 3 h, 6 h, 12 h, 24 h), by using:

$$x_t = u - (1/\alpha) \times \ln(-\ln(1 - 1/\text{RP})).$$

Subsequently, for each raingauge and each return period, a regression of rainfall quantiles over different durations has been carried out, showing best fit to the power law:  $h = a \times t^n$  (with regression parameters “ $a$ ” and “ $n$ ” estimated specifically for each raingauge). This allowed us to calculate rainfall height (i.e. rainfall rate) for 10 years return period ( $P_{\text{RP10}(i,j)}$ ) at  $j$ th rainfall durations of 30', 1 h, 2 h, 3 h, 6 h, for each  $i$ th raingauge considered (including these located closer to the larger number of debris flows occurrences during events A and B, ( $P_{\text{RP10}(j)-\text{event-A}}$ ;  $P_{\text{RP10}(j)-\text{event-B}}$ ). For sensitivity analysis purposes, calculation has also been performed with reference to other return periods.

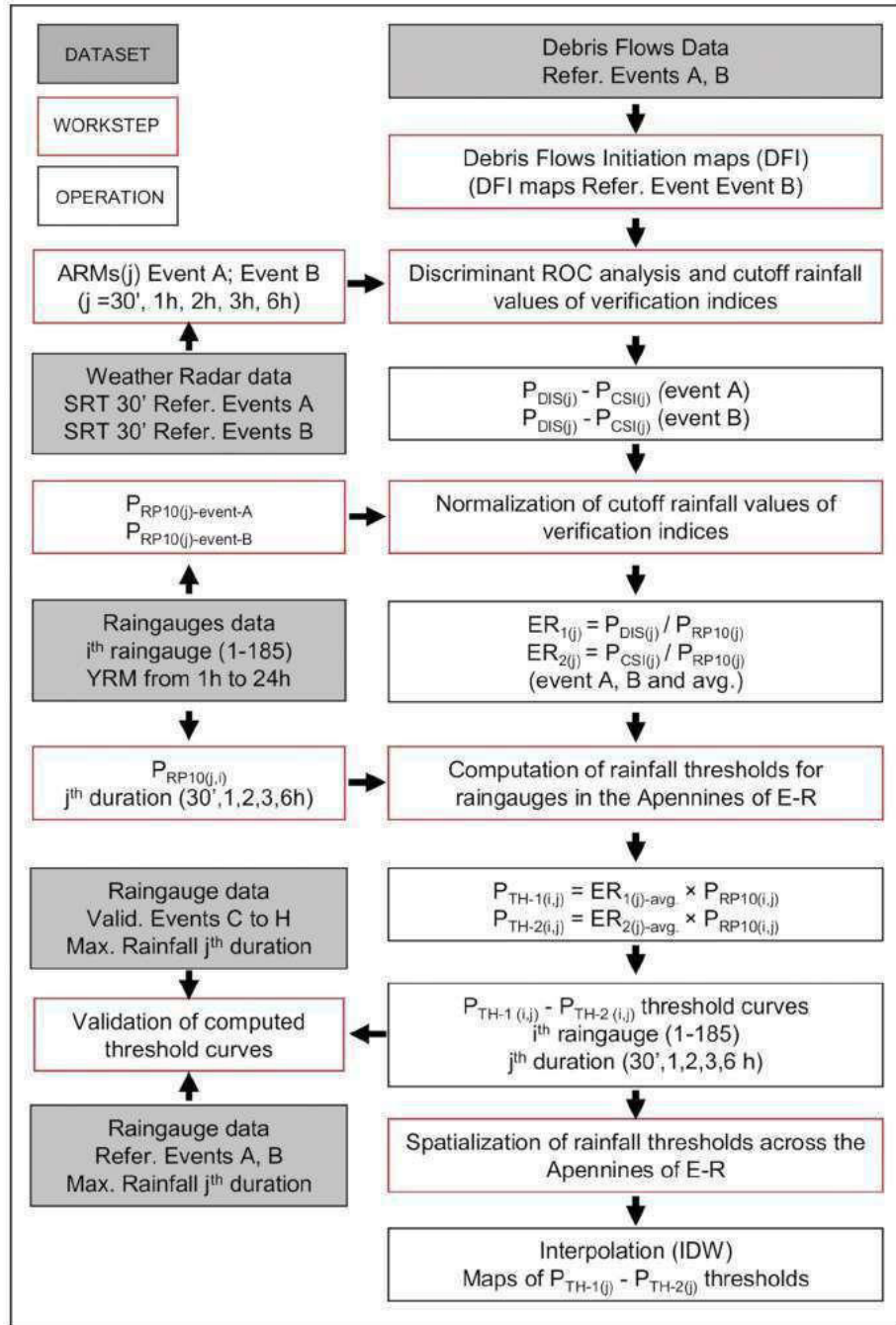


Fig. 7. Flowchart of operational procedures.

### 3.2.6. Normalization of cutoff rainfall values of verification indices

In order to introduce a normalization metrics, we have calculated the ratio (hereafter referred to “exceedance ratio” ER) between the rainfall cutoff values for the selected verification indices for  $j$ th rainfall durations (i.e.  $P_{DIS-event-A(j)}$ ,  $P_{DIS-event-B(j)}$ ) and  $P_{CSI-event-A(j)}$ ,  $P_{CSI-event-B(j)}$ ) and the rainfall rate for 10 years return period for  $j$ th rainfall duration ( $P_{RP10(j)}$ ) in raingauges of the ARPAE network. Two values of ER were calculated for each specific  $j$ th rainfall duration:

$$ER_{1(j)} = P_{DIS(j)} / P_{RP10(j)}; ER_{2(j)} = P_{CSI(j)} / P_{RP10(j)}$$

The  $ER_{1(j)}$  and  $ER_{2(j)}$  have been computed separately for event A and event B, by considering  $P_{RP10(j)}$  values for the raingauges located close to the larger number of debris flows occurrences (raingauge “Marra” for

$P_{RP10-event-A(j)}$  and raingauge “Salsominore” for  $P_{RP10-event-B(j)}$ ). The resulting values (i.e.  $ER_{1(j)-event-A}$ ;  $ER_{1(j)-event-B}$  and  $ER_{2(j)-event-A}$ ;  $ER_{2(j)-event-B}$ ) have finally been averaged ( $ER_{1(j)-avg}$  and  $ER_{2(j)-avg}$ ).

Sensitivity analysis has shown that the choice of using the  $P_{RP10(j)}$  as “normalization” metrics, rather than precipitations at different returns period, has actually some influence on the results. At the same time, the choice of using  $ER_{1(j)}$  and  $ER_{2(j)}$  of event A, or B, or averaged, influences only results at short  $j$ th rainfall durations (see Discussion section).

### 3.2.7. Computation of rainfall thresholds for all raingauges in the Apennines of Emilia Romagna

The averaged values of exceedance ratio ( $ER_{1(j)-avg}$  and  $ER_{2(j)-avg}$ ) derived by the analysis of reference events A and B, have been used as multiplier in order to extrapolate raingauge specific precipitation

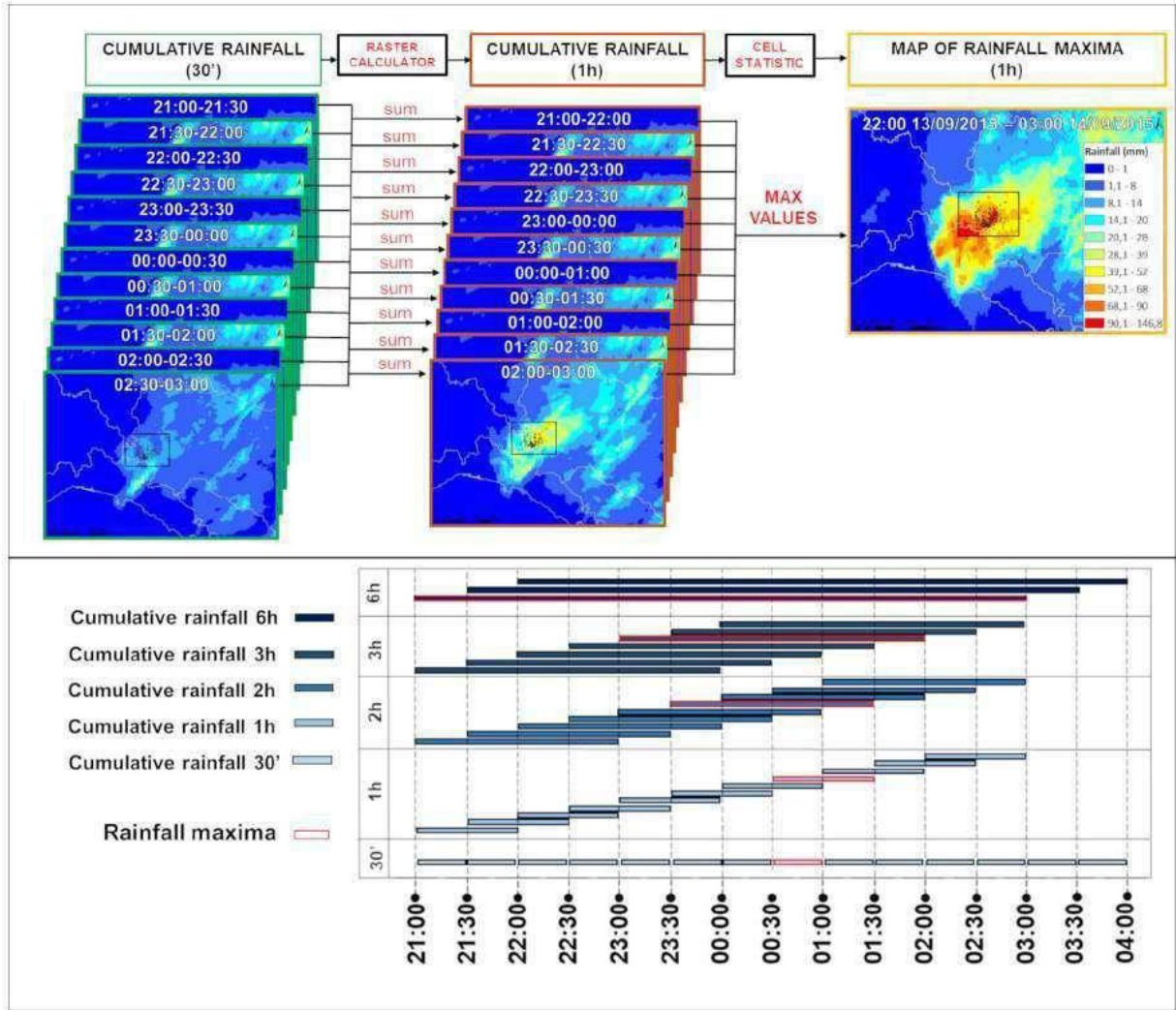


Fig. 8. Exemplification of the method used to obtain Asynchronous Rainfall Maxima maps at different rainfall durations (ARMj) during the reference rainstorm events A and B, by using a 30' moving window over which the maxima of cumulated rainfall totals at various rainfall durations (30', 1 h, 2 h, 3 h, 6 h) have been determined, for each pixel, using GIS functionalities.

thresholds for the 185 raingauges distributed across the Apennines of Emilia Romagna which are part of the ARPAE SIM network. With respect to each  $i$ th raingauge, two differentiated thresholds values have been calculated as:

$$P_{TH-1(i,j)} = ER_{1(j)} \cdot avg \times P_{RP10(i,j)}; P_{TH-2(i,j)} = ER_{2(j)} \cdot avg \times P_{RP10(i,j)}$$

where  $P_{RP10(i,j)}$  is 10 years return period rainfall calculated in each  $i$ th raingauge at a given  $j$ th rainfall duration.

The  $P_{TH-1(i,j)}$  and  $P_{TH-2(i,j)}$  of each raingauge have been calculated for  $j$ th rainfall durations of 30', 1 h, 2 h, 3 h, 6 h. On such basis, two threshold curves in a rainfall Intensity Duration plot have also been determined for each  $i$ th raingauge: a lower curve with  $P_{TH-1(i,j)}$  and an higher curve with  $P_{TH-2(i,j)}$ . By considering the minimum and maximum distribution of  $P_{TH-1(i,j)}$  and  $P_{TH-2(i,j)}$  values for all the 185  $i$ th raingauges considered, it has also been possible to extract a general exponential equation putting into relation intensity and duration ( $I D$ ).

### 3.2.8. Spatialization of rainfall thresholds across the Apennines of Emilia Romagna

Finally, the rainfall thresholds  $P_{TH-1(i,j)}$  e  $P_{TH-2(i,j)}$  for each of the 185  $i$ th raingauges, have been spatialized by inverse distance weighted method, in order to obtain maps of  $P_{TH-1(j)}$  e  $P_{TH-2(j)}$  across the Apennines of Emilia Romagna with grid cells of 500 by 500 m. We adopted

IDW because, differently from other interpolation methods (such as kriging), it maintains unaltered the values in the interpolation nodes. Moreover, we did not apply a geographically weighted regression, since unlike other authors have made for yearly rainfalls (Brunsdon et al., 1996), we considered that precipitation during rainstorms cannot be univocally related to ground elevation.

### 3.2.9. Comparison of computed rainfall thresholds with rainfall maxima during validation events

Validation of results has been performed by plotting the maximum intensity precipitations over the  $j$ th rainfall durations recorded during the validation events C to H, against the extrapolated spatialized predictive cutoff rainfall thresholds obtained for raingauges located inside the areas affected by the validation events. For a more complete picture, maximum intensities precipitations from a number of raingauges located in the reference event A and B areas have also been plotted.

## 4. Results

### 4.1. ROC analysis, cutoff rainfall values of verification indices and normalization

The ROC curves obtained by the analysis of the relationships between debris flow occurrence and rainfall peaks classes at different rainfall durations (30', 1 h, 2 h, 3 h, 6 h) during the reference event A (Parma

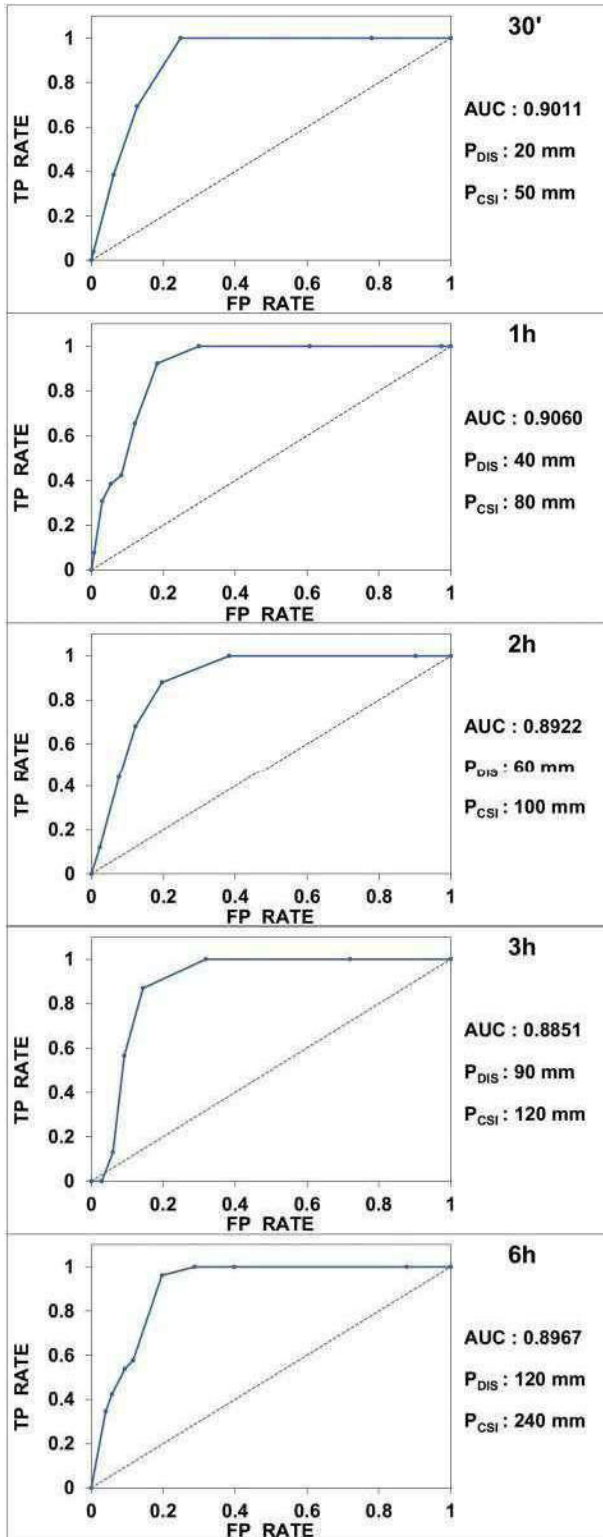


**Fig. 9.** Reference event A: ROC curves at various  $j$ th duration, with values of the Area Under the Curve (AUC) and of the cutoff rainfall values for the selected verification indices ( $P_{DIS}$  and  $P_{CSI}$ ).

2014) and reference event B (Piacenza 2015), are presented in Figs. 9 and 10.

The calculated AUC indicate a significant predictive capacity of rain fall durations ranging from 30' to 6 h. For event A, an AUC >0.9 is obtained for 30' and 1 h durations, and >0.7 for the other durations (Fig. 9). For event B the AUC is >0.9 for all rainfall durations, with slightly

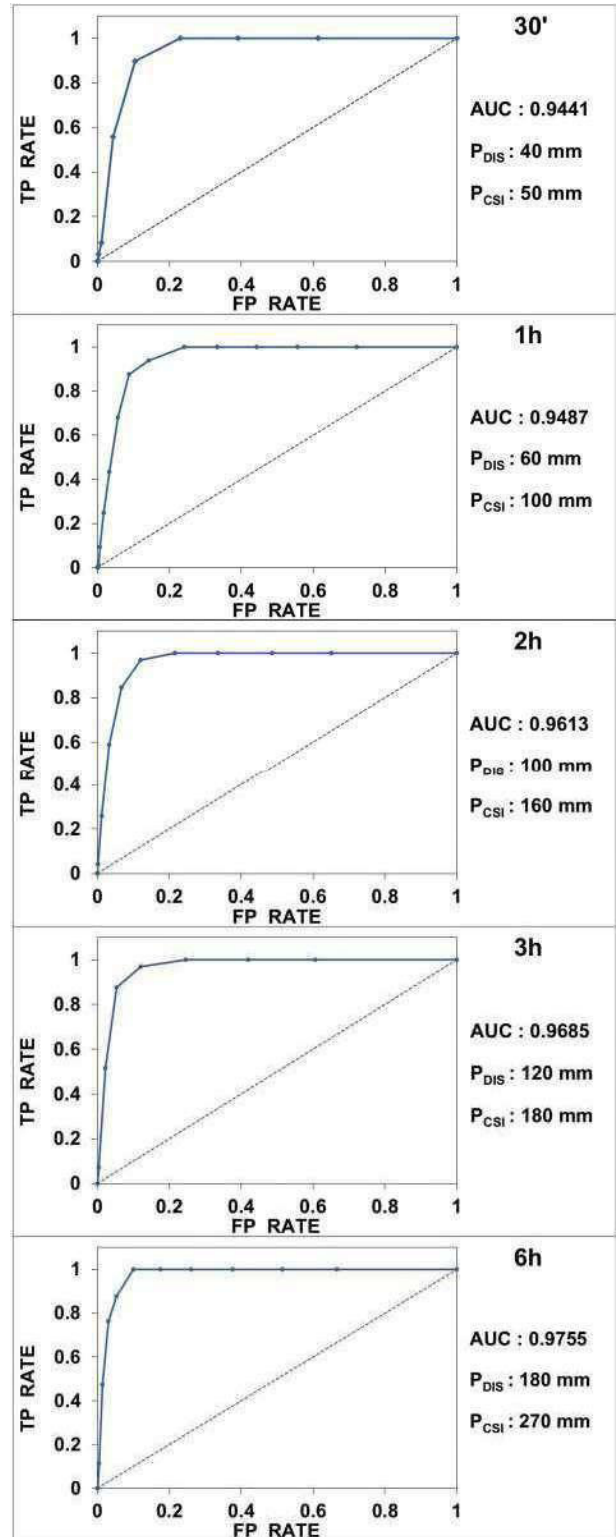


**Fig. 10.** Reference event B: ROC curves at various  $j$ th duration, with values of the Area Under the Curve (AUC) and of the cutoff rainfall values for the selected verification indices ( $P_{DIS}$  and  $P_{CSI}$ ).

higher values in the longer durations (Fig. 10). The cutoff rainfall values for the chosen verification indices ( $P_{DIS(j)}$  e  $P_{CSI(j)}$ ) differ for event A and event B (Table 4 and Fig. 11). Normalized as "exceedance ratios" ( $ER_{1(j)}$  and  $ER_{2(j)}$ ) of the 10 years return period precipitations calculated for their representative raingauges (Marra for event A and Salsominore for event B), they result of a similar order of magnitude (Table 4). The

**Table 4**  
Exceedance ratios for various  $j$ th rainfall durations ( $ER_{1(j)} = P_{DIS(j)}/P_{RP10(j)}$ ;  $ER_{2(j)} = P_{CSI(j)}/P_{RP10(j)}$ ) in reference events A and B.

$j$	Reference Event A					Reference Event B					Average exceedance ratio	
	$P_{DIS}$ (j)-event-A (mm)	$P_{CSI}$ (j)-event-A (mm)	$P_{RP10}$ (j)-event-A (mm)	$ER_1$ (j)-event-A	$ER_2$ (j)-event-A	$P_{DIS}$ (j)-event-B (mm)	$P_{CSI}$ (j)-event-B (mm)	$P_{RP10}$ (j)-event-B (mm)	$ER_1$ (j)-event-B	$ER_2$ (j)-event-B	$ER_1$ (j)-avg	$ER_2$ (j)-avg
30'	20	50	38	0.58	1.31	40	50	59	0.67	0.84	0.62	1.07
1 h	40	80	50	0.80	1.50	60	100	76	0.78	1.30	0.79	1.40
2 h	60	100	66	0.91	1.52	100	160	99	1.01	1.61	0.96	1.56
3 h	90	120	78	1.15	1.53	120	180	114	1.05	1.57	1.10	1.55
6 h	120	240	103	1.16	2.20	180	270	147	1.23	1.84	1.19	2.02

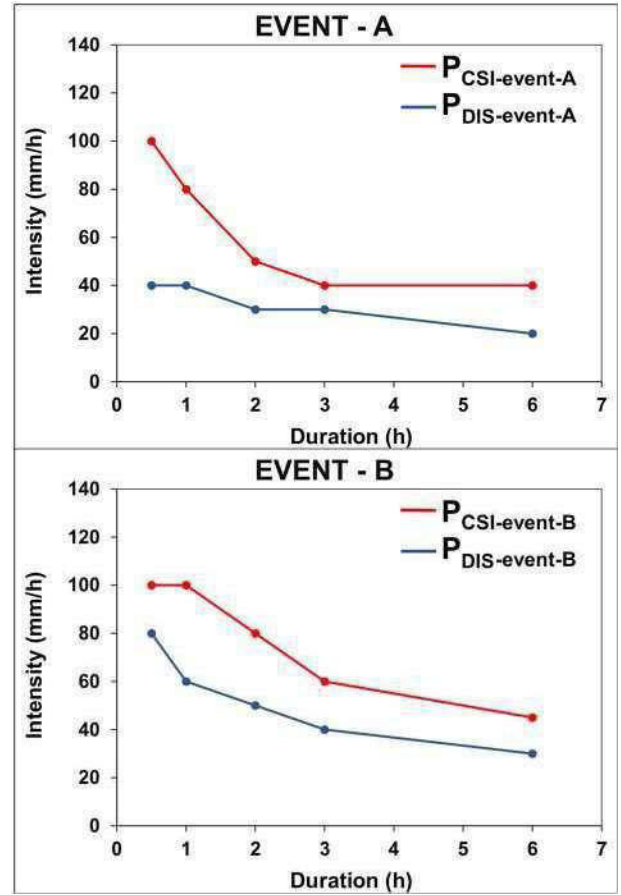


**Fig. 11.** Cutoff rainfall values (expressed as hourly intensity) for verification indices at various  $j$ th rainfall durations (30' to 6 h) ( $P_{DIS(j)}$  and  $P_{CSI(j)}$ ) for event A (raingauge Marra) and Event B (raingauge Salsominore).

averaged ER values increase with increasing rainfall duration, with  $ER_{1-avg(j)}$  ranging from 0.62 at 30' to 1.19 at 6 h, and  $ER_{2-avg(j)}$  ranging from 1.07 at 30' to 2.02 at 6 h duration.

#### 4.2. Computation and spatialization of rainfall thresholds across the Apennines of Emilia Romagna

The distribution of rainfall rate at 10 years return period ( $P_{RP10(i,j)}$ ) for 185  $i$ th raingauges for different  $j$ th rainfall durations (from 30' to 6 h) is presented in Fig. 12. The variability of  $P_{RP10(i,j)}$  values reflects the different meteorological regimes across the Apennines of Emilia Romagna. On the basis of the analysis carried out with respect to reference event A and event B, the two levels debris flow rainfall thresholds ( $P_{TH-1(j)}$  and  $P_{TH-2(j)}$ ) have been calculated of all the 185  $i$ th raingauges considered across the Apennines of Emilia Romagna, by using the formulations in Table 5. By considering the distribution of  $P_{TH-1}$  and  $P_{TH-2}$  thresholds values for the 185  $i$ th raingauges considered, the general equations linking rainfall intensity and rainfall duration presented in Table 5 have been obtained.

The spatial distribution of the computed rainfall thresholds  $P_{TH-1(j)}$  and  $P_{TH-2(j)}$  is represented in Figs. 13 and 14. Thresholds values, being computed on the basis of  $P_{RP10(i,j)}$ , are also variable over the region, with higher values in the westernmost part of the region and close to the Apennine's topographic divide, and lower values in the eastern part of the region and at lower elevations. The geographical variability of rainfall thresholds  $P_{TH-1(j)}$  e  $P_{TH-2(j)}$  is an expected consequence of the analysis approach, which was actually aimed to consider the specific climatic characteristics of the various parts of the region. This variability, as it will be further commented in the Discussion section, might help to

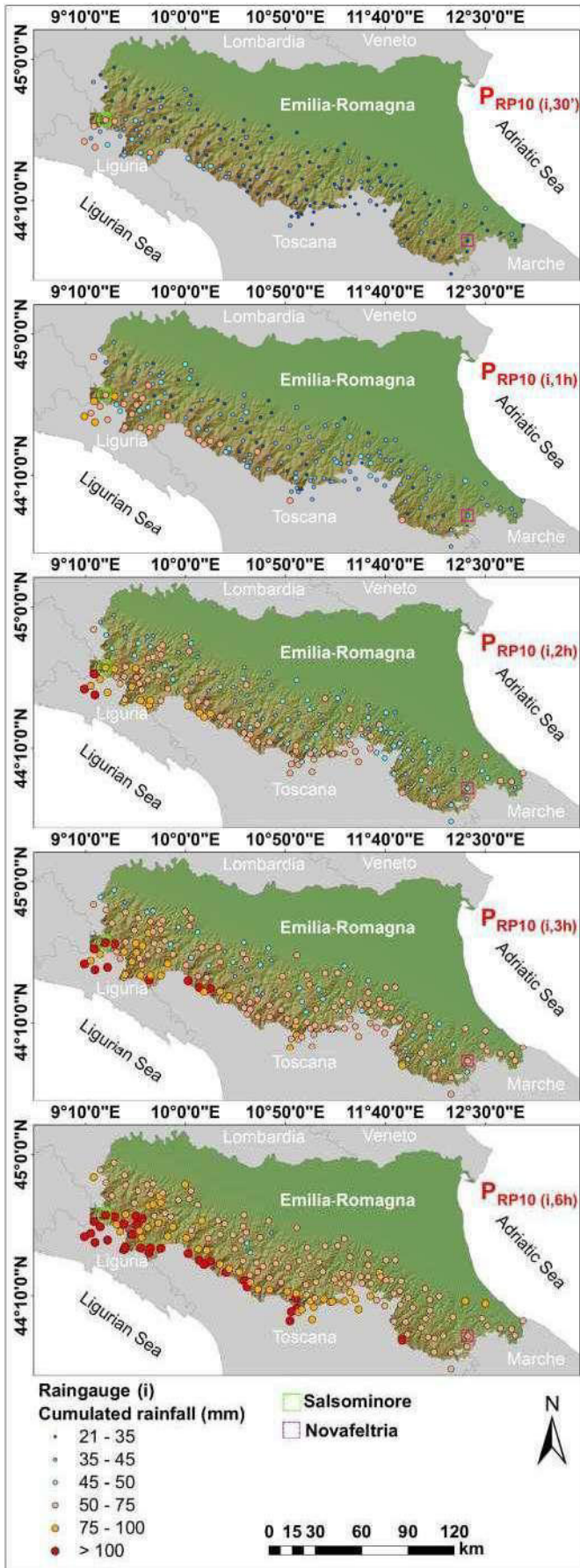


**Table 5**

General formulations of rainfall thresholds  $P_{TH-1}$  and  $P_{TH-2}$ .

Rainfall duration (j)	$P_{TH-1(j)}$	$P_{TH-2(j)}$
30'	$0.62 \times P_{RP10(j)}$	$1.07 \times P_{RP10(j)}$
1 h	$0.79 \times P_{RP10(j)}$	$1.4 \times P_{RP10(j)}$
2 h	$0.96 \times P_{RP10(j)}$	$1.56 \times P_{RP10(j)}$
3 h	$1.1 \times P_{RP10(j)}$	$1.55 \times P_{RP10(j)}$
6 h	$1.19 \times P_{RP10(j)}$	$2.02 \times P_{RP10(j)}$
General	$I = A \times D^{0.403}$ $A = 21.3 \div 71.3$	$A = 35.7 \div 119.7$

overcome the limitations of using equal thresholds all over the Apennines of Emilia Romagna as currently in use by the civil protection authorities. As an example,  $P_{TH-1}$  and  $P_{TH-2}$  thresholds for raingauge Salsominore (in the western part of the region) are in both cases higher than the thresholds at present considered for thunderstorm warning (indicated as  $P_{TH-DGR}$  of 30 mm/1 h and 70 mm/3 h in Fig. 15). Differently, in the eastern part of the region, these thresholds fall in between the  $P_{TH-1}$  and  $P_{TH-2}$  thresholds calculated for raingauge Novafeltria (Fig. 15).

#### 4.3. Comparison of rainfall thresholds and rainfall rates during validation events

The maxima rainfall intensities (at the various jth rainfall durations) recorded in the relevant raingauges during the validation events (C to H, spanning over the 1972 to 2016 period), as well as the maxima recorded during the reference events (A 2014 and B 2015) are reported in Table 6. These data have been plotted against the rainfall thresholds  $P_{TH-1(i,j)}$  and  $P_{TH-2(i,j)}$  obtained for the relevant raingauges located inside the areas affected by validation events (Fig. 16). The plots show that all the validation events C to H have been consequent to maximum rainfall rates equal or higher than the lower thresholds (i.e.  $P_{TH-1(i,j)}$ ) and that, in many cases, maximum rainfall rates during the validation events C to H were also higher than the upper thresholds (i.e.  $P_{TH-2(i,j)}$ ). These results demonstrate that the calculated thresholds are capable of discriminating the rainfall rates recorded in the past occurrence of debris flows. As it will be further evidenced in Discussion section, this gives the opportunity to use both thresholds in a multi stage warning perspective.

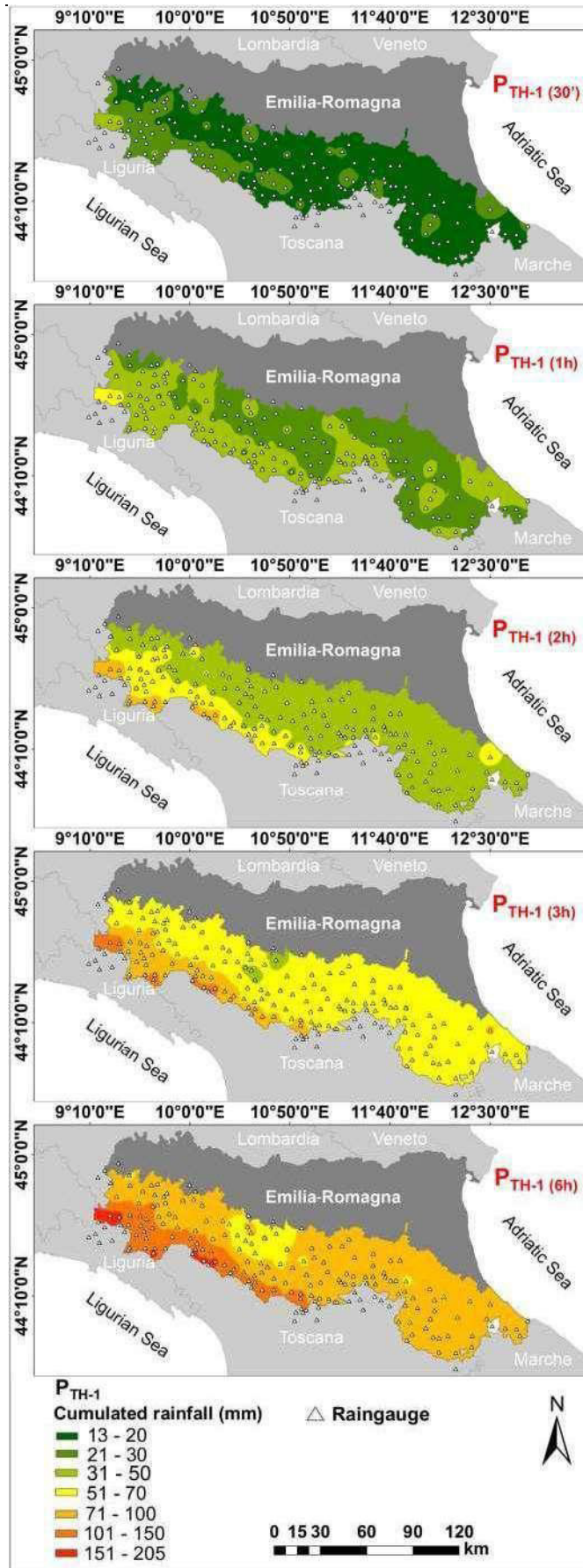
## 5. Discussion

### 5.1. Limitations and uncertainties of the adopted approach

#### 5.1.1. Limitations and uncertainties related to working hypothesis and assumptions

Like any other rainfall threshold based study, our approach has the limitation of not considering the spatial dimension of hazard. The susceptibility of slopes to debris flows (related to the topographic, geologic, geomorphic, soil, hydraulic, vegetation conditions along the streams) is equally important for debris flows hazard assessment than triggering rainfall itself. For instance, Badoux et al. (2009), evidence that sediment entrainment and bulking produced by runoff in rills and channels, transformation of shallow landslides including landslides forming within the channel bed, and the mobilization of channel sediment may be important mechanism for the formation of debris flows. In other words, if rainfall thresholds are overcome in areas with no debris flow susceptibility, then there is no hazard. Consequently, our rainfall thresholds are only one part of the analysis process required for assessing debris flow hazard at regional scale, which requires the temporal probability

**Fig. 12.** Distribution of rainfall rate with 10 years return period ( $P_{RP10}$ ) for 185 raingauges at different jth rainfall durations in the Apennines of Emilia-Romagna (coordinates: WGS84-32N).



of occurrence of rainfall thresholds to be combined with the spatial probability of occurrence of debris flows. It is also to be underlined that in principle the susceptibility of slopes to debris flows is also some how conditioning the rainfall triggering threshold. With respect to this issue, our thresholds should therefore be considered as valid for debris flows events that occur in susceptibility conditions similar to these characterizing the areas affected by reference events.

Some other working assumptions of our analysis are also subject to limitations that affect the results. For instance, we have assumed that debris flows are triggered by rainfalls only, and that a geomorphic equilibrium exists between the slope/channel bed states and precipitation runoff climatology. Our approach, for instance, does not consider the influence of (rapid) snow melt as another possible debris flows triggering factor (Cardinali et al., 2000; Hürlimann et al., 2014; Mostbauer et al., 2018). Consequently, our calculated thresholds might be too high for snow melt triggered debris flows events. This factor limits the applicability of our results to thunderstorms related debris flows in the summer to mid autumn period which are, in any case, the large majority of reported events in the Apennines of Emilia Romagna, including our reference and validation events in the 1972 to 2016 period. Moreover, our approach does not consider the fact that following a major debris flow event, some material may be left along the channels, and instability conditions may have formed along the slopes and the channels. The loose materials and the unstable slopes may fail during subsequent events with less severe rainfall conditions than those that caused the reference events we have used as basis of our analysis.

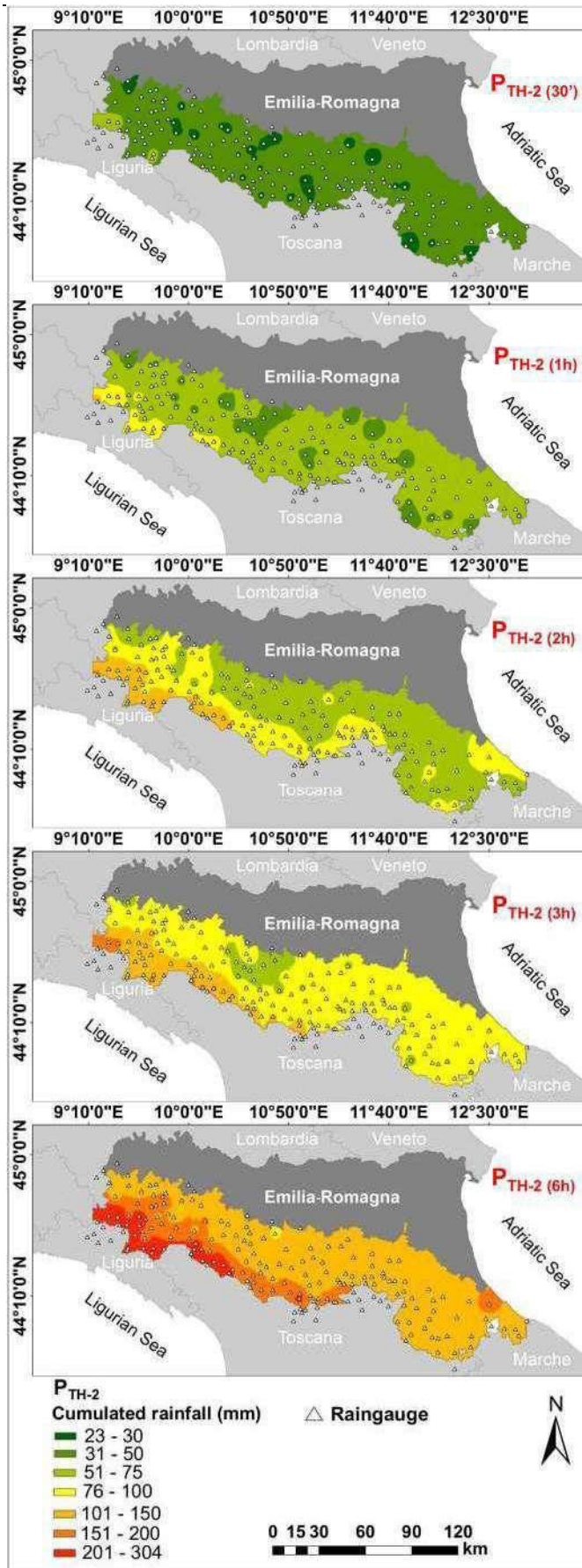
With respect to the climatological geomorphic equilibrium hypothesis, which is necessary to derive our results and that produces geographically differentiated thresholds, one limitation is that it does not account for other factors that in a given area might perturbate such equilibrium, such as for instance sudden changes in land cover or land use (e.g. due to wildfires or wood clearance) or the effects of climate variations, which in a limited number of years can actually alter the frequency of extreme events. Consequently, the precipitation expected with 10 years return period at various rainfall durations in each raingauge ( $P_{TR10(j)}$ , which has been used for calculation, normalization and extrapolation of thresholds) should actually change in the future. Also, a change in climate may also result in changes in the periods of the year when debris flow triggering conditions are possible. The incorporation of expected precipitation changes scenarios for the next decades in the calculation of thresholds has not been carried out, for the substantially different resolution of the raingauge data we have used and that of the (much coarser) rainfall changes scenarios available. Nevertheless, it should be appreciated that the  $P_{TR10(j)}$  used on this study are calculated on the basis of precipitation time series in the last 20 years, and are thus actually the best possible representative of recent climatic conditions, which, to some extent, have already been affected by ongoing climate changes.

### 5.1.2. Limitations and uncertainties related to analysis parameters (sensitivity analyses)

The analysis parameters might also have some influence on the computed rainfall thresholds. The most relevant analysis parameters are substantially the followings: (i) sampling frequency of cutoff rainfall values use to generate ROC curves; (ii) use of exceedance ratios averaged between (only) the reference event A and B; (iii) use of specific return periods rainfalls to calculate exceedance ratios.

With respect to the sampling frequency of cutoff rainfall values considered to generate ROC curves, sensitivity analysis shows that the calculated thresholds  $P_{TH1}$  (related to the DIS verification index) and  $P_{TH2}$  (related to the CSI verification index) change very little at variable

Fig. 13. Spatialization of rainfall thresholds  $P_{TH-1(j)}$  over the over the Apennines of Emilia-Romagna (coordinates: WGS84-32N).



rainfall cutoff sampling frequency. For example, results of sensitivity analysis referring to precipitation thresholds at 1 h rainfall duration using cutoff rainfall value sampling frequency variable from 1 mm to 10 mm, show that the variation of thresholds  $P_{TH1}$  and  $P_{TH2}$  is limited to few mm for all the raingauges (Fig. 17b).

With respect to the use of exceedance ratios ER averaged between the reference event A and B, sensitivity analysis shows that performing thresholds determination using the exceedance ratios averaged on event A and B (i.e.  $ER_{1(j)-avg}$  and  $ER_{2(j)-avg}$ ), rather than using the ER referring to only the reference event A (i.e.  $ER_{1(j)-event-A}$  and  $ER_{2(j)-event-A}$ ) or to only the event B (i.e.  $ER_{1(j)-event-B}$  and  $ER_{2(j)-event-B}$ ), has very limited influence for the lower  $P_{TH1}$  threshold and has some significant influence on the higher  $P_{TH2}$  threshold, but at short rainfall durations only (30' and 1 h). For instance, the sensitivity at 30' rainfall duration ranges from more than  $\pm 20$  mm in the most sensitive rain gauge (Fig. 17c) to less than  $\pm 10$  mm in the least sensitive rain gauge (Fig. 17d).

With respect to the use of rainfall rates at 10 years return period ( $P_{RP10}$ ) as normalization metrics on the basis of which calculating the exceedance ratios at various rainfall durations ( $ER_{(j)}$ ), sensitivity analysis shows that the calculated thresholds might vary over significant ranges at all  $j$ th rainfall durations by varying the return periods of normalization precipitation from 5 to 50 years. The results obtained show that the computed thresholds  $P_{TH1}$  and  $P_{TH2}$  tend to decrease at increasing return period considered and that the sensitivity is similar at all  $j$ th rainfall durations. For instance, sensitivity ranges from  $\pm 5$  mm for  $P_{TH1}$  and  $\pm 10$  mm for  $P_{TH2}$  in the most sensitive rain gauge (Fig. 17e) to less than  $\pm 2$  mm for both  $P_{TH1}$  and  $P_{TH2}$  in least sensitive rain gauge (Fig. 17f). The length of time series of yearly rainfall maxima (YRM) that has been used to assess  $P_{RP10}$  varies from 13 to 93 years depending on the specific rain gauge considered. This is not optimal and it is also a factor that has some influence on our results. However, given the circumstances, excluding from the analysis rain gauges with the shorter time series would have significantly reduced the spatial density of rain gauges for which thresholds have been calculated (and then interpolated). Moreover, rain gauges with shorter time series are actually among the ones that are now operated in the ARPAE SIM network for thunderstorms early warning: thus, excluding them from the analysis of thresholds would have inhibited the possible applications of the calculated debris flows thresholds.

## 5.2. Specificity of results and comparison with some other existing debris flows thresholds

As stated in the Methods section, our analysis approach differs from the conventional deterministic approaches adopted in literature, that generally define thresholds by enveloping cumulated rainfalls at the exact time of occurrence of events in an Intensity Duration plot. The reason for this, was that we did not have specific information on the time of occurrence of each of the debris flows occurred during the reference events of 2014 and 2015, as they all took place in unmonitored basins located all over the affected valleys. Nevertheless, it should be pinpointed that our discriminant approach does not assume that debris flows events during the reference events occurred when the rainfall intensity during the storms was at its maxima. Actually, our threshold values never correspond to the peak values recorded during these events. They are lower precipitation rates that, according to the discriminant analysis and the selected verification indices, can (probabilistically) be considered as better discriminant/forecasters of debris flow occurrence ( $P_{TH-1}$ , related to the DIS verification indices and  $P_{TH-2}$ , related to the CSI verification indices). This also implies that our analysis considers the possibility that 2014 and 2015 debris flows events

Fig. 14. Spatialization of rainfall thresholds  $P_{TH-2(j)}$  over the Apennines of Emilia-Romagna (coordinates: WGS84-32N).

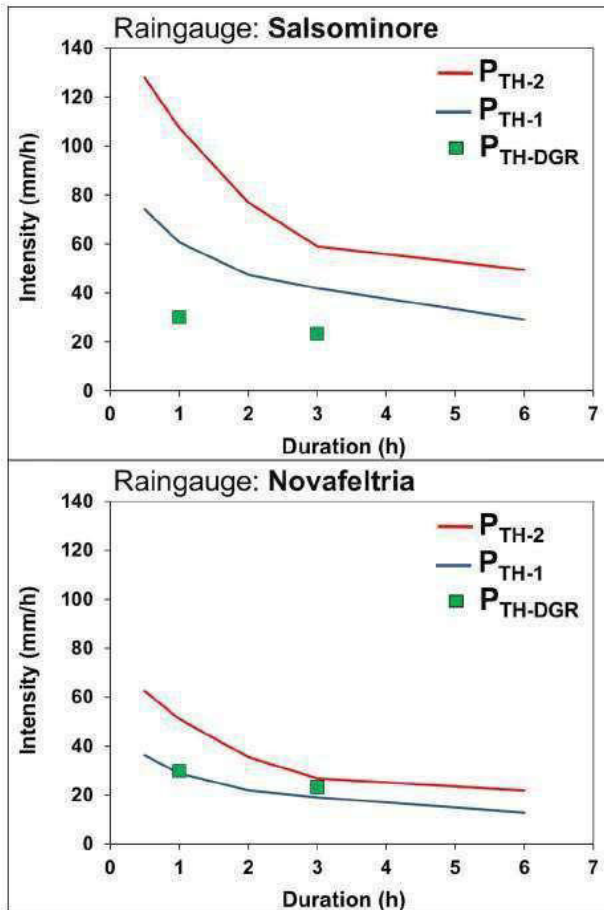


Fig. 15. Comparison between the rainfall thresholds  $P_{TH-1}$  and  $P_{TH-2}$  extrapolated for raingauges located in different areas of the Apennines of Emilia-Romagna. By reflecting different ordinary rainfall regimes, thresholds curves are significantly higher for the raingauge Salsominore than the equivalent thresholds for the raingauge Novafeltria (see Fig. 12 for location of cited raingauges).

might have occurred even before or after the maximum rainfall rates recorded. Actually, the assumption of debris flows possibly having occurred at maximum precipitation rates, has only been used to plot the

validation events (for which no radar data were available) in the Intensity Duration plots and to confront them with the calculated thresholds. Results of such a comparison, indicate that the potential risk of overestimation of thresholds is limited for the lower threshold ( $P_{TH-1}$ , related to the DIS verification index) and not high for the higher threshold ( $P_{TH-2}$ , related to the CSI verification index), since all the validation events actually lay above the  $P_{TH-1}$  threshold values and most of them also above the  $P_{TH-2}$  threshold values.

Furthermore, one of the main specificities of our results is the geographical variability of computed thresholds. As a matter of facts, our approach has been conceived to define debris flows thresholds that account for a geographical/climatic variability inside the regional study area. This is why we have normalized the thresholds computed in the two examined training case studies on the basis of their exceedance ratio with respect to precipitations at 10 years return period in each given rainfall duration considered, and we have them used the same exceedance ratio to calculate thresholds for all other raingauges in the region. Let us specify that we bear in mind the fact that debris flows are physically based processes and that, in principle, equaled all other predisposing factors, the triggering thresholds should be independent from the meteorological climatic regime of an area. But, actually, the different regional debris flows thresholds presented in literature, as well as some recent papers, evidence that there is possibly a climatic control on landslide thresholds values. Also, precipitation values recorded during past validation debris flows events, evidence a climatic control. This has led us to consider with some interest the possibility that, inside our study area region, a mid term geomorphic equilibrium along the slopes and streambeds can be reflected on differentiated debris flows triggering thresholds. The validation results indicate that the computed thresholds, despite the limitations previously discussed, can actually discriminate the past debris flow events in the Apennines of Emilia Romagna.

In comparison to debris flows thresholds reported in literature (for example, and not exhaustively, these referred to as regional and local debris flow thresholds in the review paper of Guzzetti et al., 2007), the range of variability of  $P_{TH-1}$  and  $P_{TH-2}$  thresholds (which reflects the variability of climatic regimes in the Apennines of Emilia Romagna which has been accounted for in determining thresholds) is such that the maximum values of  $P_{TH-1}$  and  $P_{TH-2}$  thresholds are actually higher than most of the thresholds in literature, while the minimum values of  $P_{TH-1}$  and  $P_{TH-2}$  thresholds are actually in line with most of the thresholds in literature (Fig. 18 and Table 7).

Table 6

Rainfall values recorded at relevant site-specific raingauges (at the various jth rainfall durations) during the reference (A, B) and validation (C to H) rainstorms events triggering debris flows in the last decades, and associated threshold values  $P_{TH-1}$  and  $P_{TH-2}$ .

Event	N° DF	Relevant raingauge	Rainfall event (mm)					$P_{TH-1}$ (mm)					$P_{TH-2}$ (mm)				
			30'	1 h	2 h	3 h	6 h	30'	1 h	2 h	3 h	6 h	30'	1 h	2 h	3 h	6 h
A	7	Calestano	19.4	36.8	58	74	116.2	20.9	33.4	50.9	66.5	90.3	36.0	59.1	82.6	93.8	153.2
A	5	Bosco di Corniglio	52.8	72.6	115.2	160	213.6	22.4	39.9	68.0	94.9	143.7	38.6	70.8	110.5	133.7	244.0
A	7	Casasevatica	13.8	27	48.4	66.2	97.2	13.4	23.3	38.6	53.0	78.2	23.2	41.3	62.7	74.7	132.7
A	7	Marra	58.2	82	132	196.6	257.8	23.6	39.7	63.7	85.9	122.8	40.7	70.3	103.5	121.1	208.4
B	2	Bobbio	18.7	30.2	58.8	77.6	94	18.6	29.3	43.8	56.7	75.5	32.2	51.9	71.2	79.8	128.1
B	3	Farini	29.8	52.4	86.2	113.4	156.2	17.7	29.4	46.5	62.2	87.7	30.6	52.1	75.6	87.7	148.8
B	21	Ferriere	54.2	87.6	129.4	146	219	24.2	38.5	58.3	76.0	102.4	41.8	68.2	94.7	107.0	173.8
B	1	Rovegno	71.4	116	142	177.4	257.4	26.6	45.3	73.5	99.8	144.2	45.9	80.3	119.5	140.6	244.8
B	59	Salsominore	57.2	107.6	151.2	201.8	294.6	37.0	60.6	94.7	125.6	174.6	63.9	107.5	153.8	177.0	296.4
B	2	Selva Ferriere	30.4	51.8	77	91.6	156.8	24.5	41.1	65.8	88.6	126.4	42.3	72.9	107.0	124.9	214.5
B	22	Trebbia Valsigara	48.6	89.6	139.8	176.6	231.2	32.4	53.6	84.4	112.6	157.9	56.0	95.0	137.2	158.6	268.0
C	13	Succiso	n.a.	97	n.a.	247	311	28.8	50.0	82.8	113.7	167.7	49.7	88.6	134.5	160.2	284.6
C	1	Ospitaletto	n.a.	58	n.a.	111.6	147.2	22.0	38.6	64.5	89.1	132.7	38.0	68.4	104.8	125.6	225.2
C	2	Lago Paduli	n.a.	102	n.a.	229.4	279	26.4	46.0	76.5	105.2	155.6	45.6	81.6	124.3	148.2	264.1
D	1	Salsomaggiore	n.a.	71	n.a.	71	112	24.6	38.1	56.3	72.4	95.2	42.5	67.6	91.5	102.0	161.5
E	1	Bosco di Corniglio	n.a.	50	n.a.	120	180	22.4	39.9	68.0	94.9	143.7	38.6	70.8	110.5	133.7	244.0
F	1	Ligonchio	n.a.	98	n.a.	196	223	23.2	38.8	61.7	82.9	117.5	40.1	68.7	100.3	116.7	199.4
G	1	Pievepelago	17	29.4	53.8	71.6	119.2	16.3	29.2	49.9	69.9	106.4	28.1	51.7	81.1	98.4	180.6
H	2	Albareto	32.8	60.2	113	135.6	145.4	32.5	51.8	78.7	102.8	139.0	56.2	91.9	128.0	144.9	236.0

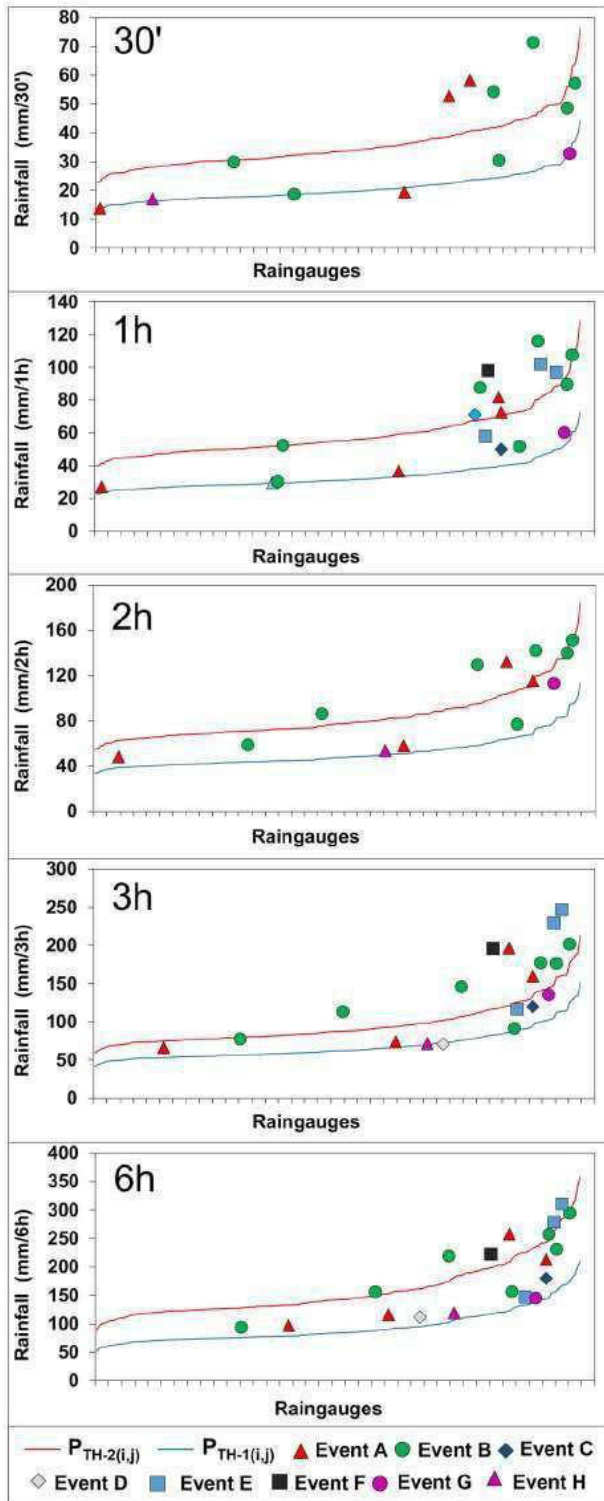


Fig. 16. Global plots of the rainfall thresholds  $P_{TH-1}$  and  $P_{TH-2}$  (at the various  $j$ th rainfall durations) for the 185 raingauges analysed across the Apennines of Emilia-Romagna (numbered and ordered from lower to higher thresholds values) and comparison with the rainfall values recorded during the rainstorms that generated debris-flows in the past decades (events A to H). Events dots show that these events have always exceeded the thresholds  $P_{TH-1}$  for all the  $j$ th rainfall durations and, in some cases, also the thresholds  $P_{TH-2}$ .

### 5.3. Possible application of results on the regional early warning system

In general, a warning system for debris flows based only on precipitation is possible but limited. Meteorological forecasts, geophones,

seismographs, runoff gauges and video cameras etc., all incorporated in a resilient system and redundant communication system may be a reasonable add on for a warning system (Badoux et al., 2009; Stähli et al., 2015). Nevertheless, the application of such approaches is necessarily site specific, and warning systems at regional scale are generally based on rainfall only (Baum and Godt, 2010).

As a matter of fact, at present, the regional early warning system for the Apennines of Emilia Romagna does not include specific rainfall threshold for debris flows. Such phenomena are generically considered as one of the possible consequence of rainstorms. Rainstorms warning thresholds have been arbitrarily defined by the National Department of Civil Protection at 30 mm/1 h and 70 mm/3 h (values that have been indicated as  $P_{TH-DGR}$  in the previous section of this paper). These thresholds are also adopted by the Civil Protection Agency of Emilia Romagna Region for the forecast and early warning procedures. One major limitation of using these thresholds with respect to debris flows is that they are fixed and equal all over the territory, and they do not consider the hypothesis that a geomorphic equilibrium exists between the climatic regime and slopes/streams dynamics in a given area. Consequently, adopting equal threshold all over the Apennines of Emilia Romagna, implies that in certain areas in the western part of the region the  $P_{TH-DGR}$  thresholds will be reached several times per year determining, however, a very limited possibility of actually triggering debris flows. At the opposite, in other areas in the eastern part of the Apennines of Emilia Romagna, the  $P_{TH-DGR}$  thresholds might actually be too high for effective debris flow warning, as the existing geomorphic equilibrium in these areas is such that even lower rainfall aliquots might trigger debris flows. Both these possibilities, of course, refer to sites where a certain degree of susceptibility to debris flows actually exists (for geologic, geomorphic, topographic, land use, etc. reasons).

Considering these potential limitations, one possible application of the debris flows thresholds defined in this study is in the frame of a multi stage warning system consisting in pre alert, alert and alarm. For instance, in areas in which the general fixed thresholds are lower than both our calculated thresholds, then the  $P_{TH-DGR}$  could be used for pre alert, the  $P_{TH-1}$  for alert and the  $P_{TH-2}$  for alarm. This could be the case, for instance, of most of the western parts of the Apennines of Emilia Romagna. Conversely, where the general fixed thresholds are higher than our lower thresholds (as in the eastern parts of the region), the  $P_{TH-1}$  could be used for pre alert, the  $P_{TH-DGR}$  for alert and the  $P_{TH-2}$  for alarm. In this way, it would be possible to mitigate the warning fatigue related to a potential large number of false alarms in the western parts of the region (potentially generating "crying wolf" phenomena) and, at the same time, have a more conservative warning system in the eastern parts of the Apennines of Emilia Romagna.

## 6. Conclusions

The research has allowed the assessment of differentiated two levels debris flows rainfall thresholds curves across the Apennines of Emilia Romagna Region. The analysis approach assumes a correlation between debris flows rainfall thresholds and rainfall regimes across the Apennine area. The method is potentially duplicable in other mountain areas where the physiographic and debris flows characteristics are similar to the ones observed in the analysed areas of the Apennines, i.e. in situations in which debris flows are triggered by mobilization of slope deposits which have a relatively little possibility to be replaced in the short term. The rainfall thresholds extrapolated at the scale of the Apennines of Emilia Romagna have been compared to rainfall data referring to other past debris flow events used for validation, showing that the calculated thresholds are capable of discriminating the rainfall rates recorded in the past occurrence of debris flows. After discussing limitations and specificity of the proposed approach and thresholds, it has been shown that our calculated thresholds can be in some cases be significantly higher than other threshold values proposed in literature. The

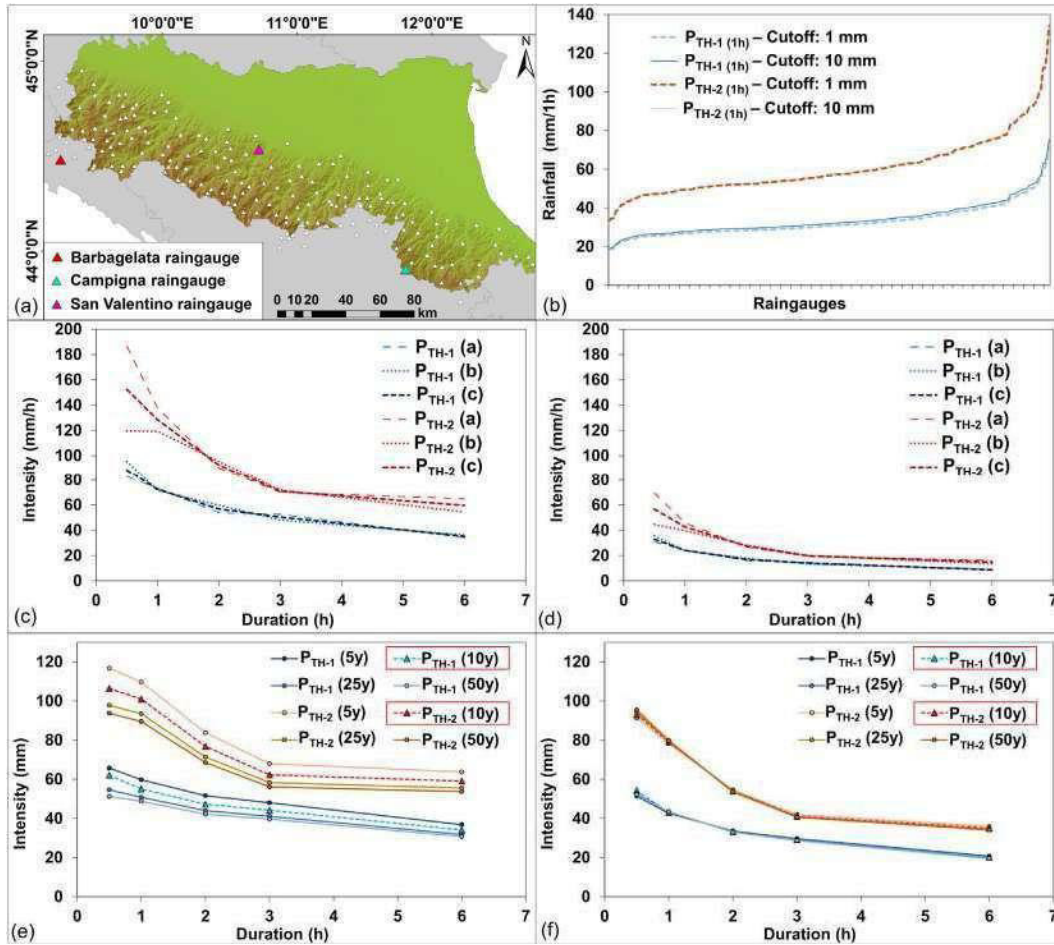


**Fig. 17.** Results of sensitivity analysis. Box-a: distribution of raingauges used for boxes c, d, e, f. (box-b) Sensitivity to changing sampling frequency of cutoff rainfall values considered to generate ROC curves for the 185 ith raingauges considered. Box-c: sensitivity of  $P_{TH-1}$  and  $P_{TH-2}$  to changing ER values for the most sensitive of the 185 ith raingauges considered (Barbagelata). Box-d: sensitivity of  $P_{TH-1}$  and  $P_{TH-2}$  to changing ER values for the least sensitive of the 185 ith raingauges considered (Campigna). Box-e: sensitivity of  $P_{TH-1}$  and  $P_{TH-2}$  to changing Return Period used to normalize threshold values, for the most sensitive of the 185 ith raingauges considered (Barbagelata). Box-f: sensitivity of  $P_{TH-1}$  and  $P_{TH-2}$  to changing Return Period used to normalize threshold values, for the least sensitive of the 185 ith raingauges considered (San Valentino). (Captions for Box-c and Box-d:  $P_{TH-1}$ (a) and  $P_{TH-2}$ (a) refer to ER values for event A;  $P_{TH-1}$ (b) and  $P_{TH-2}$ (b) refer to ER values for event B;  $P_{TH-1}$ (c) and  $P_{TH-2}$ (c) refer to averaged ER values).

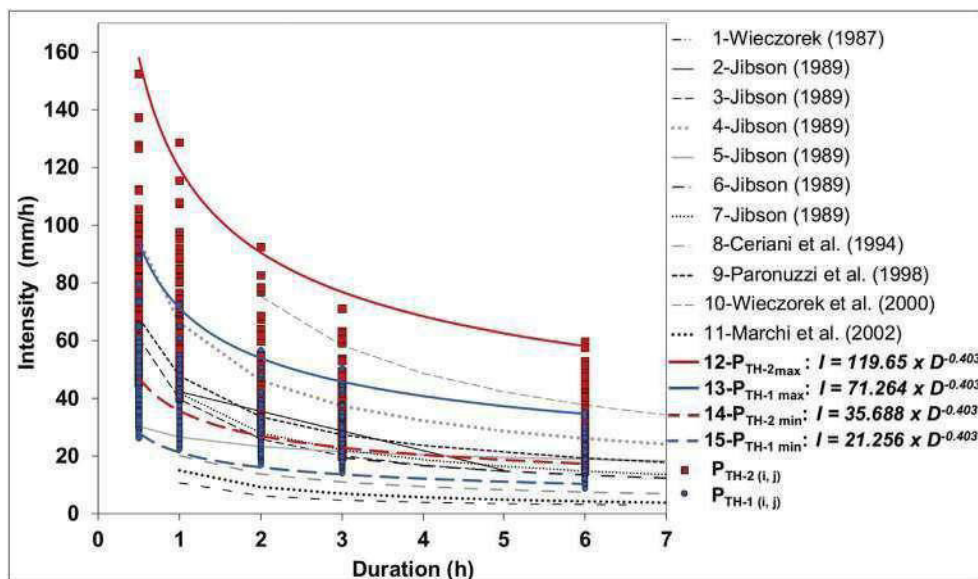


**Fig. 18.** Comparison between regional and local debris flow thresholds included in the review paper by Guzzetti et al. (2007) and the range of variability in 185 raingauges of thresholds  $P_{TH-1}$  e  $P_{TH-2}$  calculated in this study for the Apennines of Emilia-Romagna.

**Table 7**  
Comparison between regional and local debris flow thresholds included in the review paper by Guzzetti et al. (2007) and thresholds  $P_{TH1}$  e  $P_{TH2}$  calculated in this study for the Apennines of Emilia-Romagna ( $I$  = rainfall intensity in mm;  $D$  = rainfall duration in h).

Id	Source	Equation	Range	Extent	Area
1	Wieczorek (1987)	$I = 1.7 + 9 \times D^{1.00}$	$1 < D < 6.5$	Local	Central Santa Cruz Mountains, California
2	Jibson (1989)	$I = 49.11 - 6.81 \times D^{1.00}$	$1 < D < 5$	Regional	China
3	Jibson (1989)	$I = 39.71 \times D^{0.62}$	$0.5 < D < 12$	Regional	Japan
4	Jibson (1989)	$I = 66.18 \times D^{0.52}$	$0.5 < D < 12$	Regional	Puerto Rico
5	Jibson (1989)	$I = 26.51 \times D^{0.19}$	$0.5 < D < 12$	Regional	California
6	Jibson (1989)	$I = 35.23 \times D^{0.54}$	$3 < D < 12$	Regional	California
7	Jibson (1989)	$I = 41.83 \times D^{0.58}$	$1 < D < 12$	Local	Hong Kong
8	Ceriani et al. (1994)	$I = 20.1 \times D^{0.55}$	$1 < D < 1000$	Regional	Lombardy, Italy
9	Paronuzzi et al. (1998)	$I = 47.742 \times D^{0.507}$	$0.1 < D < 24$	Regional	NE Alps, Italy
10	Wieczorek et al. (2000)	$I = 116.48 \times D^{0.63}$	$2 < D < 16$	Local	Blue Ridge, Madison County, Virginia
11	Marchi et al. (2002)	$I = 15 \times D^{0.70}$	$1 < D < 30$	Local	Moscato Torrent, Italy
12	This study: $P_{TH2 \max}$	$I = 119.650 \times D^{0.403}$	$0.5 < D < 6$	Local	Apennines of Emilia-Romagna, Italy
13	This study: $P_{TH1 \max}$	$I = 71.264 \times D^{0.403}$	$0.5 < D < 6$	Local	Apennines of Emilia-Romagna, Italy
14	This study: $P_{TH2 \min}$	$I = 35.688 \times D^{0.403}$	$0.5 < D < 6$	Local	Apennines of Emilia-Romagna, Italy
15	This study: $P_{TH1 \min}$	$I = 21.256 \times D^{0.403}$	$0.5 < D < 6$	Local	Apennines of Emilia-Romagna, Italy

results can potentially be used as basis for a multi stage early warning system in civil protection procedures.

### Declaration of competing interest

The authors declare that they have no known competing financial interests or personal relationships that could have appeared to influence the work reported in this paper.

### Acknowledgements

This work was supported by the Agency for Civil Protection and Territorial Security of Emilia Romagna Region, under the framework of the partnership agreement for "Research, technical, scientific and informative activities on support to the forecast, prevention and management of hydrogeological risk 2016-2021" (scientific responsible Alessandro Corsini). During part of the research, G. Ciccacese was supported by a grant issued by the PhD Course in "Models and Methods for Material and Environmental Sciences" of the University of Modena and Reggio Emilia.

Distinct contributions: G. Ciccacese was responsible for data analysis and co wrote most of the paper; A. Corsini supervised and coordinated the research and co wrote most of the paper; M. Mulas was involved in data analyses and co wrote some parts of the paper; P. Alberoni provided radar datasets and access to raingauge data; G. Truffelli was involved during post event field surveys and data acquisition and promoted the research. The authors wish to acknowledge the constructive contribute of the anonymous reviewers for the improvement of this manuscript and, also, wish to thank the Editor for having allowed adequate time for revision.

### References

Abbate, E., Bortolotti, V., Passerini, P., Sagri, M., 1970. Introduction to the geology of the Northern Apennines. *Sediment. Geol.* 4 (3-4), 207-249.

Alberoni, P.P., Ferraris, L., Marzano, F., Nanni, S., Pelosini, R., Siccardi, F., 2002. The Italian radar network: current status and future developments. *Proceedings of ERAD 2002*. Copernicus GmbH, pp. 339-344.

Aleotti, P., 2004. A warning system for rainfall-induced shallow failures. *Eng. Geol.* 73 (3), 247-265.

APAT, 2007. Rapporto sulle frane in Italia: il Progetto IFFI: metodologia, risultati e rapporti regionali. APAT.

Bacchini, M., Zannoni, A., 2003. Relations between rainfall and triggering of debris-flow: case study of Cancia (Dolomites, Northeastern Italy). *Natural Hazards and Earth System Science* 3 (1/2), 71-79.

Badoux, A., Graf, C., Rhyner, J., Kuntner, R., McArdell, B.W., 2009. A debris-flow alarm system for the Alpine Illgraben catchment: design and performance. *Nat. Hazards* 49 (3), 517-539.

Baum, R.L., Godt, J.W., 2010. Early warning of rainfall-induced shallow landslides and debris flows in the USA. *Landslides* 7, 259-270.

Bel, C., Liébault, F., Navratil, O., Eckert, N., Bellot, H., Fontaine, F., Laigle, D., 2017. Rainfall control of debris-flow triggering in the Réal Torrent, Southern French Prealps. *Geomorphology* 291, 17-32.

Berti, M., Simoni, A., 2007. Prediction of debris flow inundation areas using empirical mobility relationships. *Geomorphology* 90, 144-161.

Berti, M., Martina, M.L.V., Franceschini, S., Pignone, S., Simoni, A., Pizzolo, M., 2012. Probabilistic rainfall thresholds for landslide occurrence using a Bayesian approach. *Journal of Geophysical Research: Earth Surface* 117 (F4).

Bertolini, G., Corsini, A., Tellini, C., 2017. Fingerprints of large-scale landslides in the landscape of the Emilia Apennines. In: Soldati, M., Marchetti, M. (Eds.), *Landscapes and Landforms of Italy*. World Geomorphological Landscapes. Springer, Cham, pp. 215-224.

Bettelli, G., De Nardo, M.T., 2001. Geological outlines of the Emilia Apennines (Northern Italy) and introduction to the formations surrounding the landslides which resumed activity in the 1994-1999 period. *Quad. Geol. Appl.* 8 (1), 1-26.

Brunetti, M.T., Peruccacci, S., Rossi, M., Luciani, S., Valigi, D., Guzzetti, F., 2010. Rainfall thresholds for the possible occurrence of landslides in Italy. *Nat. Hazards Earth Syst. Sci.* 10 (3), 447-458.

Brunson, C., Fotheringham, S., Charlton, M., 1996. Geographically weighted regression modelling spatial non-stationarity. *Geogr. Anal.* 28, 281-289.

Caine, N., 1980. The rainfall intensity: duration control of shallow landslides and debris flows. *Geografiska Annaler A* 62, 23-27.

Calcaterra, D., Parise, M., Palma, B., Pelella, L., 2000. The influence of meteoric events in triggering shallow landslides in pyroclastic deposits of Campania, Italy. *Landslides in Research, Theory and Practice: Proceedings of the 8th International Symposium on Landslides held in Cardiff on 26-30 June 2000*. Thomas Telford Publishing, pp. 1-209.

Cannon, S.H., 1988. Regional rainfall-threshold conditions for abundant debris-flow activity. *Landslides, Floods, and Marine Effects of the Storm of January 3-5, 1982, in the San Francisco Bay Region, California*, pp. 35-42.

Cannon, S.H., Gartner, J.E., 2005. Wildfire-related debris flow from a hazard perspective. *Debris-flow Hazards and Related Phenomena*. Springer Berlin Heidelberg, pp. 363-385.

Cardinali, M., Ardizzone, F., Galli, M., Guzzetti, F., Reichenbach, P., 2000. Landslides triggered by rapid snow melting: the December 1996-January 1997 event in Central Italy. *Proceedings 1st Plinius Conference on Mediterranean Storms*: Bios, Cosenza, 2000, pp. 439-448.

Cardinali, M., Galli, M., Guzzetti, F., Ardizzone, F., Reichenbach, P., Bartocchini, P., 2006. Rainfall induced landslides in December 2004 in south-western Umbria, central Italy: types, extent, damage and risk assessment. *Natural Hazards and Earth System Science* 6 (2), 237-260.

Ceriani, M., Lauzi, S., Padovan, N., 1994. Rainfall thresholds triggering debris-flows in the alpine area of Lombardia Region, central Alps-Italy. *Proc. Man and Mountain, I Conv. Intern. Per la Protezione e lo Sviluppo dell'ambiente montano, Ponte di legno (BS)*, pp. 123-139.

Chow, V.T., Maidment, D.R., Mays, L.W., 1988. *Applied Hydrology*. McGraw-Hill, New York.

Ciccacese, G., Corsini, A., Pizzolo, M., Truffelli, G., 2016. Debris flows in Val Nure and Val Trebbia (N Apennines) during the September 2015 alluvial event in Piacenza Province (Italy). *Rendiconti Online Società Geologica Italiana* 41, 127-130.

Ciccacese, G., Corsini, A., Alberoni, P.P., Celano, M., Fornasiero, A., 2017. Using weather radar data (rainfall and lightning flashes) for the analysis of debris flows occurrence in Emilia-Romagna Apennines (Italy). *Workshop on World Landslide Forum*. Springer, Cham, pp. 437-448.

Corominas, J., Moya, J., 1996. Historical landslides in the Eastern Pyrenees and their relation to rainy events. *Landslides*. AA Balkema, Rotterdam, pp. 125-132.

Corominas, J., Moya, J., 1999. Reconstructing recent landslide activity in relation to rainfall in the Llobregat River basin, Eastern Pyrenees, Spain. *Geomorphology* 30 (1), 79-93.

Corsini, A., Mulas, M., 2016. Use of ROC curves for early warning of landslide displacement rates in response to precipitation (Piagneto landslide, Northern Apennines, Italy). *Landslides* 14, 1241.

- Corsini, A., Ciccacese, G., Diena, M., Truffelli, G., Alberoni, P.P., Amorati, R., 2017. Debris Flows in Val Parma and Val Baganza (Northern Apennines) during the 12–13th October 2014 alluvial event in Parma Province (Italy). *Italian Journal of Engineering Geology and Environment* 29–38.
- Crosta, G., 1998. Regionalization of rainfall thresholds: an aid to landslide hazard evaluation. *Environ. Geol.* 35 (2–3), 131–145.
- Crosta, G., Frattini, P., 2001. Rainfall thresholds for the triggering of soil slips and debris flows. *Mediterranean Storms 2000. GNDCI*, pp. 463–488.
- Deganutti, A.M., Marchi, L., Arattano, M., 2000. Rainfall and debris-flow occurrence in the Moscardo basin (Italian Alps). *Proceedings, Second International Conference on Debris-flow Hazard Mitigation: Mechanics, Prediction, and Assessment*. AA Balkema, Rotterdam, pp. 67–72.
- Destro, E., Marra, F., Nikolopoulos, E.I., Zoccatelli, D., Creutin, J.D., Borga, M., 2017. Spatial estimation of debris flows-triggering rainfall and its dependence on rainfall return period. *Geomorphology* 278, 269–279.
- Di Baldassarre, G., Brath, A., Montanari, A., 2006. Reliability of different depth-duration-frequency equations for estimating short-duration design storms. *Water Resour. Res.* 42 (12).
- Fiorillo, F., Wilson, R.C., 2004. Rainfall induced debris flows in pyroclastic deposits, Campania (southern Italy). *Eng. Geol.* 75 (3), 263–289.
- Floris, M., Mari, M., Romeo, R.W., Gori, U., 2004. Modelling of landslide-triggering factors—a case study in the northern Apennines, Italy. *Engineering Geology for Infrastructure Planning in Europe* 745–753.
- Gariano, S.L., Brunetti, M.T., Iovine, G., Melillo, M., Peruccacci, S., Terranova, O., Vennari, C., Guzzetti, F., 2015. Calibration and validation of rainfall thresholds for shallow landslide forecasting in Sicily, southern Italy. *Geomorphology* 228, 653–665.
- Genevois, R., Tecca, P.R., Berti, M., Simoni, A., 2000. Debris flows in the Dolomites: Experimental data from a monitoring system. *Proc., 2nd Int. Conf. on Debris Flow Hazards and Mitigation*, pp. 283–292.
- Giannechini, R., 2005. Rainfall Triggering Soil Slips in the Southern Apuan Alps (Tuscany, Italy).
- Giannechini, R., 2006. Relationship between rainfall and shallow landslides in the southern Apuan Alps (Italy). *Natural Hazards and Earth System Science* 6 (3), 357–364.
- Giannechini, R., Galanti, Y., D'Amato Avanzi, G., 2012. Critical rainfall thresholds for triggering shallow landslides in the Serchio River Valley (Tuscany, Italy). *Nat. Hazards Earth Syst. Sci.* 12 (3), 829–842.
- Govi, M., Mortara, G., Sorzana, P.F., 1985. Eventi idrologici e frane. *Geologia Applicata e Idrogeologia* 20 (2), 395–401.
- Gregoretto, C., Dalla Fontana, G., 2007. Rainfall threshold for the initiation of debris flows by channel-bed failure in the Dolomites. *Debris-flow Hazards Mitigation: Mechanics, Prediction, and Assessment. Proceedings of the 4th International Conference on Debris-Flow Hazards Mitigation* 4, pp. 11–21.
- Guadagno, F.M., 1991. Debris flows in the Campanian volcanoclastic soils. *Slope Stability Engineering Developments and Applications: Proceedings of the International Conference on Slope Stability Organized by the Institution of Civil Engineers and held on the Isle of Wight on 15–18 April 1991*. Thomas Telford Publishing, pp. 125–130.
- Gumbel, E.J., 1958. *Statistics of Extremes*. 375 pp. Columbia Univ. Press, New York.
- Guzzetti, F., Peruccacci, S., Rossi, M., Stark, C.P., 2007. Rainfall thresholds for the initiation of landslides in central and southern Europe. *Meteorol. Atmos. Phys.* 98 (3), 239–267.
- Guzzetti, F., Peruccacci, S., Rossi, M., Stark, C.P., 2008. The rainfall intensity–duration control of shallow landslides and debris flows: an update. *Landslides* 5 (1), 3–17.
- Hungr, O., Evans, S.G., Bovis, M.J., Hutchinson, J.N., 2001. A review of the classification of landslides of the flow type. *Environmental & Engineering Geoscience* 7 (3), 221–238.
- Hürimann, M., Abancó, C., Moya, J., Vilajosana, I., 2014. Results and experiences gathered at the Rebaixader debris-flow monitoring site, Central Pyrenees, Spain. *Landslides* 11, 939–953.
- Innes, J.L., 1983. Debris flows. *Prog. Phys. Geogr.* 7 (4), 469–501.
- Jibson, R.W., 1989. Debris flows in southern Puerto Rico. *Geol. Soc. Am. Spec. Pap.* 236, 29–56.
- Marchi, L., D'Agostino, V., 2004. Estimation of debris-flow magnitude in the eastern Italian Alps. *Earth Surf. Process. Landforms* 29, 207–220.
- Marchi, L., Arattano, M., Deganutti, A.M., 2002. Ten years of debris-flow monitoring in the Moscardo Torrent (Italian Alps). *Geomorphology* 46 (1), 1–17.
- Marra, F., Nikolopoulos, E.I., Creutin, J.D., Borga, M., 2014. Radar rainfall estimation for the identification of debris-flow occurrence thresholds. *J. Hydrol.* 519, 1607–1619.
- Marra, F., Destro, E., Nikolopoulos, E.I., Zoccatelli, D., Dominique Creutin, J., Guzzetti, F., Borga, M., 2017. Impact of rainfall spatial aggregation on the identification of debris flow occurrence thresholds. *Hydrol. Earth Syst. Sci.* 21 (9), 4525–4532.
- Martelloni, G., Segoni, S., Fanti, R., Catani, F., 2012. Rainfall thresholds for the forecasting of landslide occurrence at regional scale. *Landslides* 9 (4), 485–495.
- Mathew, J., Babu, D.G., Kundu, S., Kumar, K.V., Pant, C.C., 2014. Integrating intensity–duration-based rainfall threshold and antecedent rainfall-based probability estimate towards generating early warning for rainfall-induced landslides in parts of the Garhwal Himalaya, India. *Landslides* 11 (4), 575–588.
- Moratti, L., Pellegrini, M., 1977. Alluvioni e dissesti verificatisi nel settembre 1972 e 1973 nei bacini dei fiumi Secchia e Panaro (Province di Modena e Reggio Emilia). *Bollettino della Associazione Mineraria Subalpina*, Anno XIV, N.2, pp. 323–374.
- Mostbauer, K., Kaita, R., Prenner, D., Hrachowitz, M., 2018. The temporally varying roles of rainfall, snowmelt and soil moisture for debris flow initiation in a snow-dominated system. *Hydrol. Earth Syst. Sci.* 22 (6), 3493–3513.
- Mulas, M., Ciccacese, G., Ronchetti, F., Truffelli, G., Corsini, A., 2018. Slope dynamics and streambed uplift during the Pergalla landslide reactivation in March 2016 and discussion of concurrent causes (Northern Apennines, Italy). *Landslides* 15 (9), 1881–1887.
- Nikolopoulos, E.I., Crema, S., Marchi, L., Marra, F., Guzzetti, F., Borga, M., 2014. Impact of uncertainty in rainfall estimation on the identification of rainfall thresholds for debris flow occurrence. *Geomorphology* 221, 286–297.
- Nikolopoulos, E.I., Borga, M., Creutin, J.D., Marra, F., 2015. Estimation of debris flow triggering rainfall: influence of rain gauge density and interpolation methods. *Geomorphology* 243, 40–50.
- Ochoa-Rodríguez, S., Wang, L.P., Willems, P., Onof, C., 2019. A review of radar-raingauge data merging methods and their potential for urban hydrological applications. *Water Resour. Res.* 55, 6356–6391.
- Papani, G., Sgavetti, M., 1977. Aspetti geomorfologici del bacino del T. Ghiara (Salsomaggiore Terme, Pr) susseguenti all'evento del 18-09-1973. *Bollettino della Associazione Mineraria Subalpina* 14 (3–4), 610–628.
- Paronuzzi, P., Cocco, A., Garlatti, G., 1998. Eventi meteorici critici e debris flows nei bacini montani del Friuli. *L'Acqua, Sezione I/Memorie* 6, 39–50.
- Pasquali, G., 2003. *La Trebbia del 25 Settembre 1953*, in cento anni di storia bobbiese 1903–2003 (Editore Amici di San Colombano).
- Peruccacci, S., Brunetti, M.T., Gariano, S.L., Melillo, M., Rossi, M., Guzzetti, F., 2017. Rainfall thresholds for possible landslide occurrence in Italy. *Geomorphology* 290, 39–57.
- Piacentini, D., Troiani, F., Daniele, G., Pizzolo, M., 2018. Historical geospatial database for landslide analysis: the Catalogue of Landslide Occurrences in the Emilia-Romagna Region (CLOCKER). *Landslides* 15, 811–822.
- Pignone, S., Del Maschio, L., Pizzolo, M., Gozza, G., 2005. Determinazione di soglie pluviometriche per innesco di fenomeni franosi nell'Appennino Settentrionale—Report nell'ambito della convenzione tra ARPA—Servizio Idrometeorologico Regionale e Servizio Geologico Sismico e dei Suoli Regionale per il supporto alle attività del centro funzionale.
- Pignone, F., Rebor, N., Silvestro, F., Castelli, F., 2010. GRISO—Rain, CIMA Research Foundation, Savona, Italy, Operational Agreement 778/2009 DPC-CIMA, Year-1 Activity Report 272/2010 353 pp., 2010. (in Italian).
- Pizzolo, M., Del Maschio, L., Gozza, G., Pignone, S., 2008. Determinazione di soglie pluviometriche per l'innesco di frane in Emilia-Romagna. *Il Geologo dell'Emilia-Romagna* 29, 21–27.
- Ronchetti, F., Borgatti, L., Cervi, F., Lucente, C.C., Veneziano, M., Corsini, A., 2007. The Valoria landslide reactivation in 2005–2006 (Northern Apennines, Italy). *Landslides* 4 (2), 189–195.
- Rossetti, G., Tagliavini, S., 1977. L'alluvione ed i dissesti provocati nel bacino del Torrente Enza dagli eventi meteorologici del Settembre 1972 (Province di Parma e Reggio Emilia). *Bollettino della Associazione Mineraria Subalpina* 14 (3–4), 561–603.
- Scorpio, V., Crema, S., Marra, F., Righini, M., Ciccacese, G., Borga, M., Cavalli, M., Corsini, A., Marchi, L., Surian, N., Comiti, F., 2018. Basin-scale analysis of the geomorphic effectiveness of flash floods: a study in the northern Apennines (Italy). *Sci. Total Environ.* 640, 337–351.
- Segoni, S., Lagomarsino, D., Fanti, R., Moretti, S., Casagli, N., 2015. Integration of rainfall thresholds and susceptibility maps in the Emilia Romagna (Italy) regional-scale landslide warning system. *Landslides* 12 (4), 773–785.
- Stähli, M., Sättele, M., Huggel, C., Mcardell, B.W., Lehmann, P., Van Herwijnen, A., Berne, A., Schleiss, M., Ferrari, A., Kos, A., Or, D., Springman, S.M., 2015. Monitoring and prediction in early warning systems for rapid mass movements. *Nat. Hazards Earth Syst. Sci.* 15, 905–917.
- Swets, J.A., 1988. Measuring the accuracy of diagnostic systems. *Science* 240 (4857), 1285–1293.
- Takahashi, T., 1991. Mechanics and the existence criteria of various types of flows during massive sediment transport. In: Armanini, A., Di Silvio, G. (Eds.), *Fluvial Hydraulics of Mountain Region*. Springer-Verlag, Germany, pp. 267–278.
- Tavagnini, S., 1989. Osservazioni sui dissesti nel bacino del T. Parma conseguenti all'evento meteorico del 16 ottobre 1980. In: Alifracco, G., Tomasi, P. (Eds.), *L'acqua negata, il dilemma d'oggi tra logica umana e idrogeologica*, Parma, pp. 249–286.
- Trigila, A., Iadanza, C., Bussetini, M., Lastoria, B., Barbano, A., Munafò, M., 2015. Dissesto idrogeologico in Italia: pericolosità e indicatori di rischio. *Rapporto* 233, 2015.
- Underwood, S.J., Schultz, M.D., Berti, M., Gregoretto, C., Simoni, A., Mote, T.L., Saylor, A.M., 2016. Atmospheric circulation patterns, cloud-to-ground lightning, and locally intense convective rainfall associated with debris flow initiation in the Dolomite Alps of northeastern Italy. *Nat. Hazards Earth Syst. Sci.* 16, 509–528.
- Wieczorek, G.F., 1987. Effect of rainfall intensity and duration on debris flows in central Santa Cruz Mountains, California. *Rev. Eng. Geol.* 7, 93–104.
- Wieczorek, G.F., Morgan, B.A., Campbell, R.H., 2000. Debris flow hazards in the Blue Ridge of Central Virginia. *Environ. Eng. Geosci.* 6, 3–23.
- Zêzere, J.L., Trigo, R.M., Trigo, I.F., 2005. Shallow and deep landslides induced by rainfall in the Lisbon region (Portugal): assessment of relationships with the North Atlantic Oscillation. *Natural Hazards and Earth System Science* 5 (3), 331–344.